Journal of Environmental Management, Volume 390, August 2025, Article number 126223
DOI: 10.1016/j.jenvman.2025.126223

Life cycle analysis of ammonia-driven calcium looping processes for post-combustion CO_2 capture in NGCC power plants

Yawen Zheng[a,b], Song He[b,c,d*], Jianhui Liu[a], Junyao Wang[e,f], Mingming Zhu[d*], Guang Yang[a], Wenxiang Wang[a]

[a.] *China Shenzhen Gas Corporation Ltd. Shenzhen, 518040, P.R. China*

[b.] *Collaborative Innovation Institute of Carbon Neutrality and Green Development, Guangdong University of Technology, No.100 Waihuan Xi Road, Guangzhou, 510006, China*

[c.] *School of Ecology, Environment and Resources, Guangdong University of Technology, No.100 Waihuan Xi Road, Guangzhou, 510006, China*

[d.] *Faculty of Engineering and Applied Sciences, Cranfield University, Cranfield, Bedfordshire, MK43 0AL, United Kingdom*

[e.] *School of Material and Energy, Guangdong University of Technology, Guangzhou, 510006, China*

[f.] *Guangdong Provincial Key Laboratory of Functional Soft Matter, Guangzhou, 510006, China*

Submitted to "*Journal of Environmental Management*"

[*] Corresponding author. Address: Guangdong University of Technology, No.100 Waihuan Xi Road, Guangzhou 510006, China. Email address: hesong@gdut.edu.cn (Song He).

[*] Corresponding author. Address: Cranfield University, Cranfield, Bedfordshire, MK43 0AL, United Kingdom. Email address: Mingming.Zhu.152@cranfield.ac.uk (Mingming Zhu).

Published by Elsevier. This is the Author Accepted Manuscript issued with: Creative Commons Attribution License (CC:BY 4.0).
The final published version (version of record) is available online at DOI:10.1016/j.jenvman.2025.126223. Please refer to any applicable publisher terms of use.

Abstract: Integrating calcium looping (CaL) based carbon capture and storage (CCS) technology with an existing natural gas combined cycle (NGCC) power plants offers a promising solution for low-carbon energy production. This work introduces a novel NH_3-driven CaL process for retrofitting NGCC plants. The economic performance and environmental impacts of the process were analyzed through life cycle analysis and compared with those of conventional oxy-fuel CaL and solar-driven CaL technologies. Results indicate that, the NH_3-driven CaL demonstrates with a very low energy penalty of only 2.6 points, while the solar-driven CaL method faces a 14-points energy penalty. From an environmental perspective, the NH_3-driven CaL method, with considering various ammonia sources, significantly impacts the environment more than oxy-fuel and solar-driven methods, with global warming potential values of 207.7 (oxy-fuel), 170.7 (solar), and 197.6~258.8 g CO_2-eq/kWh (green NH_3). Economically, based on an annual operation time of 4000 hours of NGCC, the solar-driven CaL system has the lowest Life Cycle Cost of GHG Removed (*LCOR*) at 247.7 \$/t CO_2. With anticipated reductions in ammonia prices to 240 \$/t in 2050, the NH_3-driven CaL system is expected to gain a significant advantage in economic at 46.5 \$/t CO_2 when natural gas price is 0.6 \$/Nm^3. And it is important to pay attention the clean production process of ammonia to reduce its impact on the environment.

Key words: Ammonia, Post-combustion CO_2 capture, Calcium looping, Natural gas combined cycle, Life cycle analysis

Nomenclature

AP, kg SO_2-eq	Acidification Potential	LHV_{NG}, MW	Lower heating value of natural gas
ASU	Air separation unit	LHV_{NH3}, MW	Lower heating value of NH_3
CaL	Calcium looping	*LCOR*, \$/t CO_2	Life Cycle Cost of GHG Removed
CCR, %	CO_2 capture ratio	*n, years*	Equipment operating life
CEPCI	Chemical engineering plant cost index	$n_{CO2,f}$, mol/s	Mole flow of CO_2 in flue gas
		$n_{CO2,esf}$, mol/s	Mole flow of carbon content in energy supply fuel
$C_{E\text{-}CaL}$, M\$	Cost of calcium looping unit		
$C_{E\text{-convective}}$, M\$	Cost of convective pass	*NGCC*	Natural gas combined cycle
$C_{E\text{-Indirect calciner}}$, M\$	Cost of indirectly heated	PCC	Post-combustion capture

	calciner	PED, MJ	Primary Energy Demand
$C_{\text{E-Carbonator}}$, M$	Cost of carbonator	PESR	Primary energy saving ratio
$C_{\text{E-Combustor}}$, M$	Cost of combustor	POFP, kg NMVOC-eq	Photochemical Ozone Formation Potential
CF	Capacity factor		Work consumption of air separation unit
CRF	Capital recovery factor	P_{ASU}, MW	
COR, $/t CO_2	cost of CO_2 removed		Work consumption of compressors
$CO_{2,\text{cap}}$, kg/s	CO_2 emission carbon capture power plants	P_{comps}, MW	Net output power
		P_{net}, MW	Power generation in gas turbines
$CO_{2,\text{ref}}$, kg/s	CO_2 emission from reference power plants	P_{GT}, MW	Work consumption of pumps
		P_{pump}, MW	Power generation in steam turbines
DPC, M$	Direct plant cost	P_{ST}, MW	
EC, M$	Equipment cost	$Q_{\text{solar receive}}$, MW	heat received by the solar field
EP, kg PO_4-eq	Eutrophication Potential	*r*	discount factor
ET, CTU_e	Potential Ecotoxicity	RI, kg PM2.5-eq	Respiratory Inorganics
f	Scale factor	*S*	Scale of the equipment
FCI, M$	Fixed capital investment	ST	steam turbine
GHG, kg/MWh	life cycle greenhouse gas emissions	WU, kg	Water Use
		Greeks	
GT	gas turbine	α	Heat transfer surfaces
GWP, kg CO_2-eq	Global Warming Potential	$\Delta\eta$	Efficiency penalty
HRSG	Heat recovery steam generator	η_{NH3}	Power generation efficiencies of NH_3-based system
HT, CTU_h	Human toxicity		
I, M$	Cost of the equipment	η_{p}	Power generation efficiency
IPC, M$	indirect plant cost	Subscripts	
LCA	Life cycle assessment	*i*	Serials number
LCC, M$	life cycle cost	r	Reference system
LCCA	Life cycle cost assessment	w	With CO_2 capture
LCOE, $/MWh	Levelized Cost of Energy	wo	Without CO_2 capture

1. Introduction

Natural gas combined cycle (NGCC) power plants play a critical role in global efforts to reduce carbon emissions. NGCC technology, which efficiently integrates gas and steam turbines, offers a lower carbon footprint compared to coal-fired power generation, with carbon emission intensities typically around 350-400 g CO_2/kWh—approximately 50-60% lower than coal-fired plants [1]. Despite this improvement, NGCC plants still contribute significantly to global CO_2 emissions, accounting for about 22% of electricity sector emissions globally [2]. As the world moves toward carbon neutrality, NGCC power plants must adopt advanced CO_2 mitigation technologies to further reduce their carbon intensity, ensuring they can continue to play a critical role in the energy transition toward cleaner and more sustainable power generation.

For reducing CO_2 in NGCC power plants, post-combustion CO_2 capture is seen as the best option for upgrading existing plants. Calcium Looping (CaL) technology, which captures CO_2 after combustion, has been widely studied because the materials needed for solid adsorbents are easy to find and cheap [3-6]. The CaL process has been successfully validated across bench-scale, pilot-scale, and demonstration-scale facilities ranging from 1 kWth to 20 MWth [7-10], reaching a technology readiness level (TRL) of 6-7 [9, 10]. And the main challenges of applying CaL technology to NGCC plants are the capacity loss of absorbents and calcium carbonate sintering at high temperatures [11]. However, current implementations remain at the demonstration stage of the CaL process and have not yet been practically integrated into operational power plants. For the integration of CaL with NGCC plants, existing research has identified two primary integration approaches: hot-end and tail-end [12]. In the hot-end setup, CO_2 is taken directly from the hot exhaust gas of the gas turbine, and the cleaned flue gas is then sent to the heat recovery steam generator (HRSG). This strategy, while effective, introduces an energy penalty ranging between 5.0% and 10.8% [12-15]. In contrast, the tail-end configuration captures CO_2 from the lower-temperature flue gas after it passes through the HRSG. While this method allows for easier retrofitting of existing NGCC plants without major modifications, it comes with a slightly higher energy penalty, typically between 10.6% and 12.0% [12, 16, 17]. Despite this, the tail-end configuration offers a more flexible solution for existing plants, making it a viable option despite its greater efficiency loss compared to the hot-end strategy.

In the tail-end calcium looping configuration, oxy-fuel combustion is typically employed to supply heat for the calcination process. However, the production of pure oxygen for oxy-fuel

combustion is energy-intensive, with air separation units (ASUs) accounting for approximately 40% of the total energy consumption and 15% of the total plant investment [18-20]. To mitigate the energy burden associated with air separation, solar-driven calcination has also gained attention as a promising alternative [21-25]. The integration of solar energy with calcium looping carbon capture systems primarily falls into two categories: one involves using solar energy to assist the steam cycle of power plants [26], while the other provides direct heating for the calciner [27, 28]. Zhai et al. [26] conducted a comparative study on these two integration methods, focusing on solar heating for coal power steam cycles versus direct heating of the calciner. Their findings indicated that the latter approach incurs a lower efficiency penalty. Additionally, due to the intermittent nature of solar energy, existing research has proposed the inclusion of solid storage tanks to ensure stable operation of the carbon capture system over daily or weekly cycles [28-30]. Colelli et al.[31] conducted an life cycle assessment (LCA) on calcium looping with concentrated solar power for the calcination process. Their results indicated a moderate environmental impact, with calcium looping thermochemical energy storage technology producing lower equivalent CO_2 emissions (24 kg/MWh) compared to other energy storage options, such as molten salt-based solar facilities (40 kg/MWh).

However, existing research presents several challenges. On the one hand, while solar-assisted calcium looping avoids the CO_2 capture demand for energy supply fuels, its instability poses challenges for the stable operation of the capture unit. To address this gap, this paper introduces a novel concept of ammonia-driven CaL post-combustion CO_2 capture technology, specifically applied to NGCC power plants. Ammonia is an excellent renewable energy storage medium, and has garnered significant attention as a zero-carbon fuel and hydrogen carrier, but no studies have yet combined ammonia with calcium looping capture technology. The novel system uses ammonia as the energy source for calcium looping and recovers the heat released during the carbonation process to drive ammonia pyrolysis, avoiding the inefficiencies associated with large temperature differentials in direct water heating. On the other hand, although using renewable energy avoids the CO_2 capture demand for energy supply fuels, the environmental impacts during the renewable energy utilization period and the economic feasibility of the corresponding integration methods are also critically important, but there is a lack of comprehensive comparison regarding the environmental impact and economic performance from life cycle point of view among different energy supply methods in CaL technologies.

In addition to introducing the novel system, this paper evaluates various calcium looping capture

technologies powered by both fossil and renewable energy sources from a life cycle environmental and economic perspective. Following the introduction, Section 2 describes the model of various calcium looping capture technologies in detail. Section 3 introduces the analysis methods employed in this study, including energy analysis, LCA, and life cycle cost assessment (LCCA). Section 4 presents a comprehensive discussion of the results, comparing the performance of different calcium looping capture systems, assessing the environmental impact based on various ammonia sources, and analyzing the influence of ammonia and natural gas prices on the economic viability of each technology. It is expected the outcomes would shed light on the design of cost-effective CaL based technologies for retrofitting existing NGCC power plants.

2. Model description

2.1 Natural gas combined cycle (NGCC) power plant

The 180 MW natural gas combined cycle (NGCC) power plant, situated in China, is illustrated in Fig. 1. The system consists of three main components: a gas turbine (GT), a heat recovery steam generator (HRSG), and a steam turbine (ST). The GT model employed in this configuration is the PG9171E. As depicted in Fig. 1, compressed air and natural gas are fed into the combustion chamber, where they combust to drive the GT and generate mechanical power. The high-temperature exhaust gases exiting the GT are directed to the HRSG, where they produce steam to power the ST, thereby generating additional electricity. After passing through the ST, the steam is condensed, pressurized, and recirculated into the HRSG to recover residual heat from the exhaust gases, creating a continuous cycle. The HRSG in this NGCC plant operates under dual-pressure conditions without reheating. To enhance power output, supplementary water is heated in the HRSG and then fed into the low-pressure section of the ST. Furthermore, the ST is equipped with a heating extraction port, allowing steam to be diverted for use as a thermal energy source in external systems.

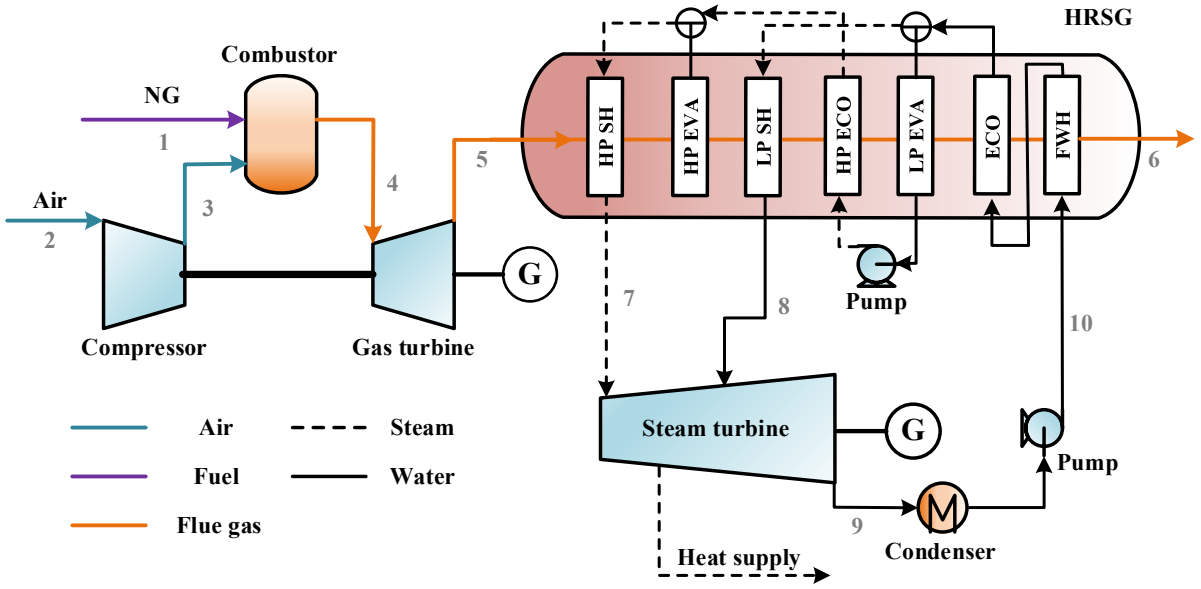

Fig.1 Flow sheet of the NGCC power plant (NG: Natural Gas, FWH: Feed Water Heater, ECO: Economizer, LP EVA: Low Pressure Evaporator, HP ECO: High Pressure Economizer, LP SH: Low Pressure Superheater, HP EVA: High Pressure Evaporator, HP SH: High Pressure Superheater)

2.2 NGCC with oxy-fuel combustion calcium looping process (CaL-OXY)

For NGCC power plants, calcium looping (CaL) technology can be integrated through two primary strategies: tail-end and hot-end configurations. These approaches differ primarily in the point at which flue gas is treated. In the tail-end configuration, flue gas exiting the HRSG is directed to the carbonator. Conversely, the hot-end configuration diverts medium-temperature flue gas from the gas turbine outlet to the carbonator. Owing to its enhanced CO_2 capture efficiency, the hot-end integration method has garnered significant attention in recent studies [14, 15, 32, 33], as shown in Fig. 2, which serves as a case study in this work. CaL technology utilizes CaO as a high-temperature sorbent to capture CO_2 from flue gas via a carbonation reaction between CaO and CO_2. Following this, the sorbent is regenerated in a calciner at elevated temperatures. A common approach to supplying the necessary heat for regeneration involves combusting fuel with pure oxygen produced by an air separation unit (ASU). The high-temperature CO_2 stream exiting the calciner, along with the decarbonized flue gas from the carbonator, is channeled through a heat recovery steam generator (HRSG). Within the HRSG, the sensible heat is harnessed to generate steam, which drives a steam turbine for additional power generation. Furthermore, the exothermic heat released during the carbonation reaction is utilized to further heat the working fluid through the pipes arranged on the furnace wall. After heat recovery, the CO_2 is compressed and prepared for storage.

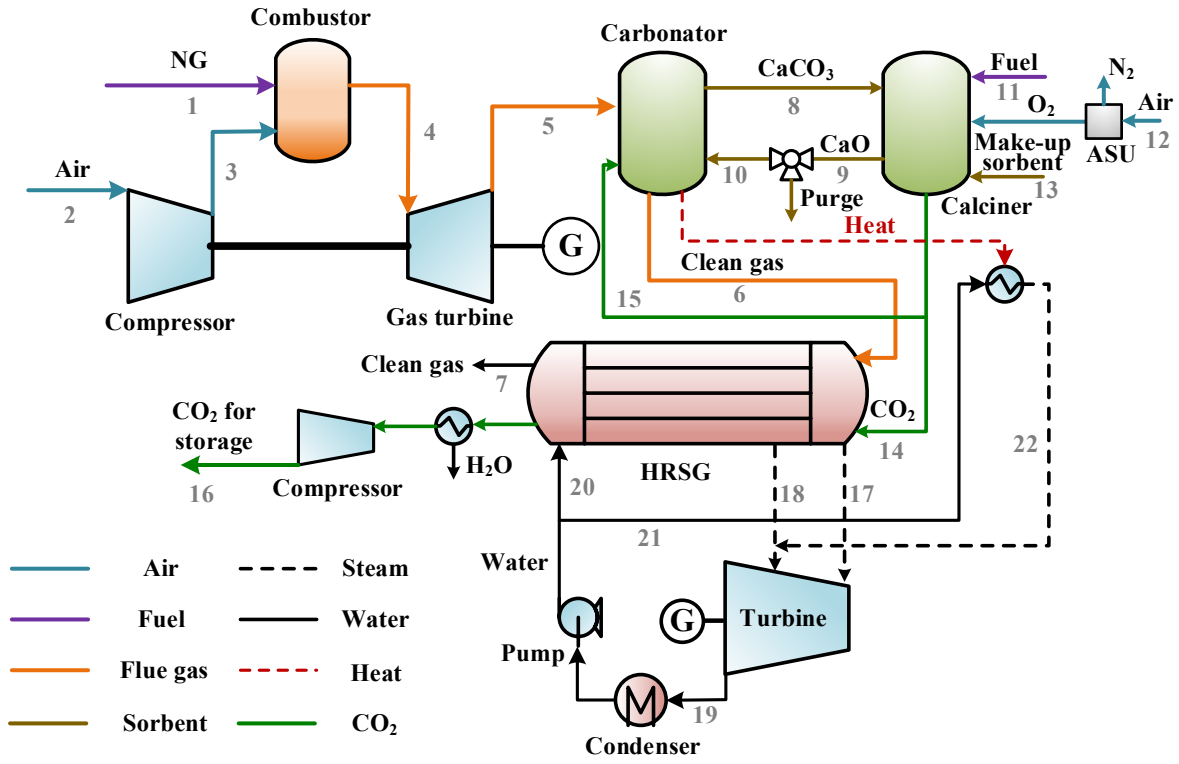

Fig.2 Flow sheet of the CaL-OXY system

2.3 NGCC with solar driven calcium looping process (CaL-SOL)

Fig.3 shows the flow sheet of the NGCC with a solar-driven calcium looping process. A solar field is used to supply high-temperature heat for the calcination process. To ensure the stable operation of the capture unit, a solid storage system should be implemented to maintain performance during periods without solar energy. In the day mode, the system utilizes solar irradiation and serve as thermal energy storage, and in the night mode, the system releases the chemical energy from the carbonation reaction and operate without solar irradiation. The daytime is assumed to be 12 hours. The size of the solid storage tanks are calculated based on methods outlined in the literature [30], ensuring that the solar carbon capture system can operate stably over a 24-hour period. Additionally, the sensible heat from the gases exiting the carbonator and calciner can be utilized to generate steam, which drives the steam turbine for power generation.

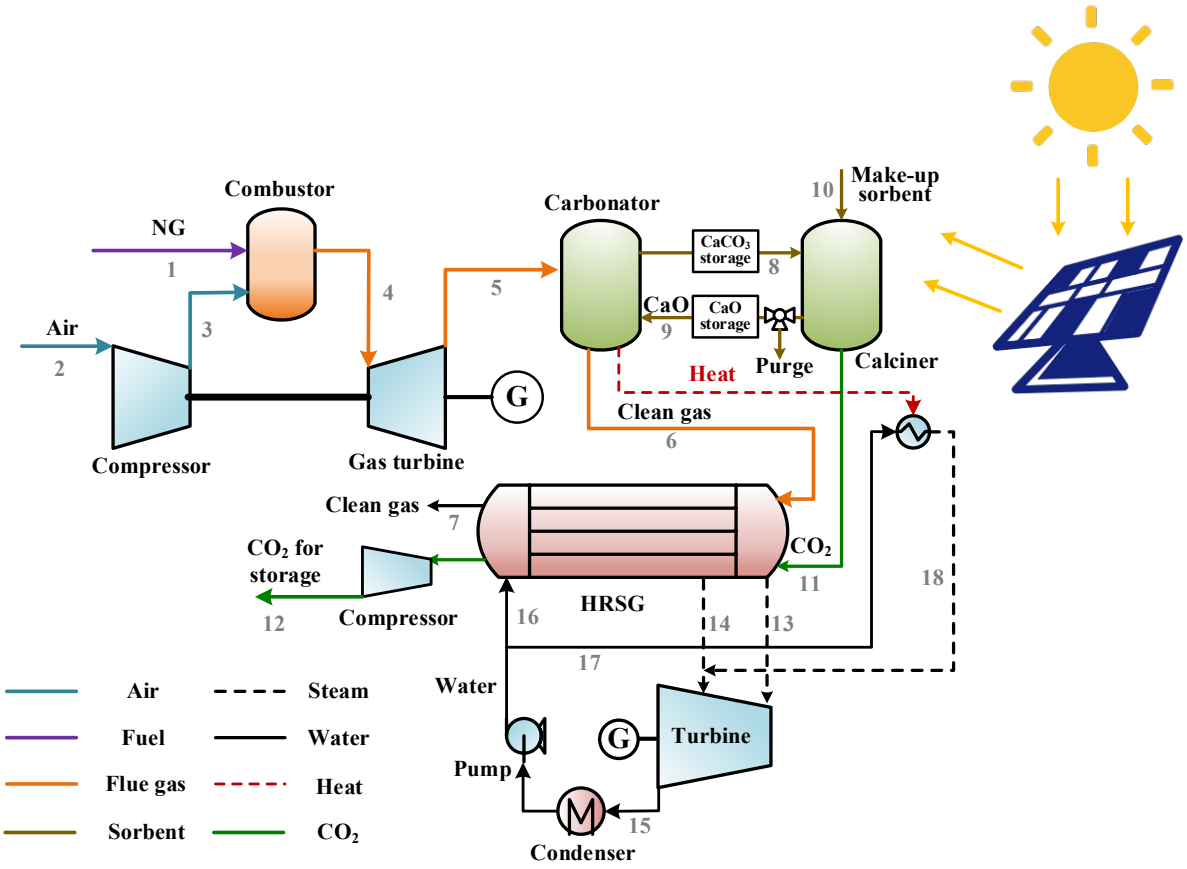

Fig.3 Flow sheet of the CaL-SOL system

2.4 NGCC with ammonia driven calcium looping process (CaL-NH_3)

While the hot-end configuration offers better energy efficiency for NGCC power plants compared to the tail-end approach, it involves substantial changes to the existing plant setup, making it less practical for real-world use. For this reason, the study focuses on the tail-end integration method and introduces a novel carbon capture process driven by ammonia, as illustrated in Fig.4. In this CaL-NH_3 system, flue gas from the NGCC plant, after being cooled, enters the carbonator for CO_2 absorption. Because the flue gas has a low CO_2 concentration and is at a lower temperature, a larger portion of its heat is transferred to the incoming gas stream. The carbonator operates endothermically, eliminating the need to preheat the flue gas. The heat recovered from the decarbonized flue gas is then utilized for two purposes: cracking NH_3 and preheating the flue gas after carbonation. In the cracker, NH_3 from storage is compressed and decomposed using a catalyst. The resulting products are mixed with compressed air and directed to the combustor. Meanwhile, the solid $CaCO_3$ formed in the carbonator is transported to the calciner, where it regenerates into CaO and releases CO_2. The heat required for calcination is supplied by the high-temperature combustion products from the $NH_3/H_2/N_2$ combustor.

After providing heat for calcination, these combustion products expand in the gas turbine. The remaining heat from the exhaust gas and the CO_2 released in the calciner is recovered in the HRSG2 unit. Additionally, the effectiveness of CaO as a sorbent decreases over multiple carbonation-calcination cycles. To address this, a small portion of the regenerated CaO is removed after calcination, and fresh $CaCO_3$ is added to maintain sorbent performance. Fig.5 schematically illustrates the heat transfer method between key components of the system: the carbonator and cracker, as well as the calciner and combustor. The high-temperature flue gases from the carbonator and combustor respectively pass through external flue channels of the cracker and calciner, where heat is transferred through metal walls to the reaction chambers to provide thermal energy for ammonia cracking and calcination reactions.

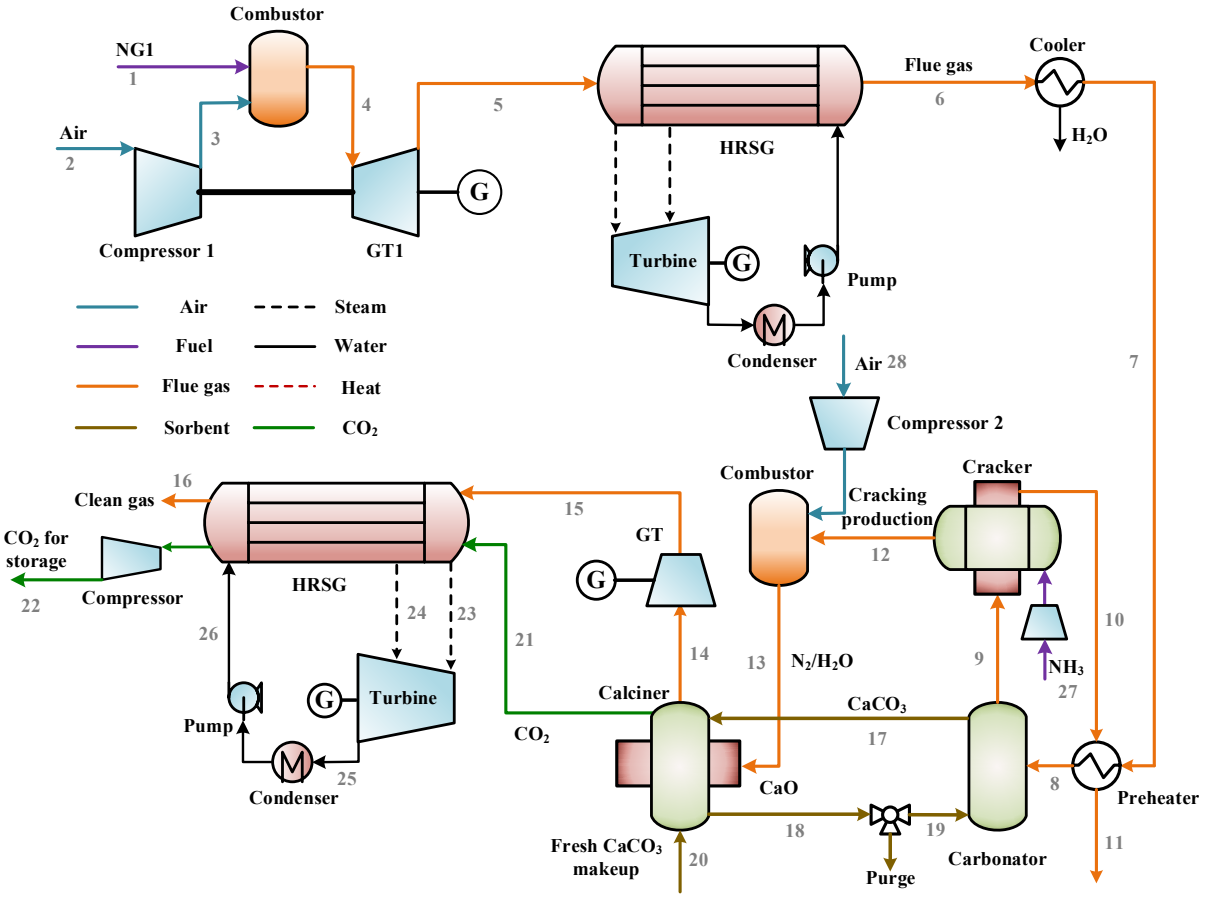

Fig.4 Flow sheet of the CaL-NH_3 system

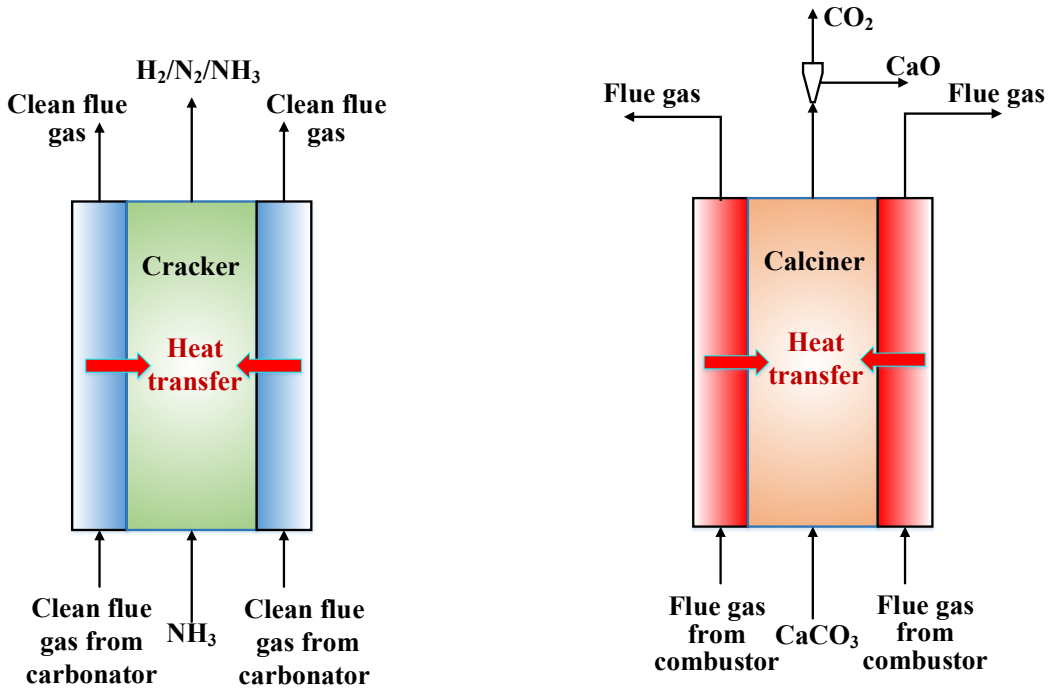

(a) Carbonator and cracker (b) Combustor and calciner

Fig.5 Heat transfer approach between reactors in the CaL-NH_3 system

2.5 Simulation

The simulations of the three CO_2 capture technologies were conducted using Aspen Plus v11.0. For property calculations, the PR-BM method was applied globally, while the STEAMNBS method was specifically used to analyze water and vapor properties in the steam cycle. To reduce computational complexity, the following assumptions were incorporated: (1) the system operates at steady state; (2) fresh make-up solids and ammonia inputs were simplified to $CaCO_3$ and NH_3, respectively; (3) gas-solid separation was assumed to be an ideal process; and (4) pressure losses and heat dissipation were disregarded. Detailed operational parameters for the three cases are summarized in Table 1. The supplementary document includes the validation results for the model.

Table 1 Main operating parameters in the proposed and reference systems

Items	Description
Feedstocks	
Natural gas input	Molar fraction: CH_4 (91.1%), C_2H_6 (6.0%), C_3H_8 (2.14%), C_4H_{10} (0.66%), N_2 (0.05%), CO_2 (0.04%), O_2 (0.01); Lower heating value (LHV): 49.44 MJ/kg; Temperature and pressure: 25 ℃ and 24.7 bar [34].
NH_3 input	100% NH_3; LHV: 18.50 MJ/kg; Temperature and pressure: 4 ℃ and 1.013 bar [35].
Solid make up	100% $CaCO_3$; Temperature of fresh make-up solids: 25 ℃, make-up ratio: 2.0% [21, 36].

Base NGCC power plant [34]	
Air compression	Outlet pressure: 12 bar; Isentropic efficiency: 0.85.
Gas turbine	Inlet temperature: 1100 ℃; Isentropic efficiency: 0.92.
HRSG	Steam parameters: 56/5.6 bar, 527℃.
Flue gas	Temperature of flue gas treated: 40 ℃.
CaL units	
Carbonator	Carbonator pressure: 1.013 bar; Carbonator temperature: 600 ℃ [13, 15]; Average CaO conversion: 0.2 [37, 38]; Inlet flue gas temperature: 550℃(CaL-OXY and CaL-SOL), 370 ℃ (CaL-NH_3).
Calciner	Calcination temperature: 900 ℃; Pressure: 1.013 bar.
HRSG2	Same with HRSG in the base NGCC power plant.
ASU	Cryogenic distillation technology; Electricity consumption: 180 kWh/t O_2; Purity of O_2: 95% [39, 40].
Other processes	
Ammonia cracking	Cracking temperature: 400 ℃; Cracking pressure: 12 bar [41] [42]
Gas turbine for NH_3 cases	Inlet temperature: 1100 ℃ [41]; Exhaust pressure: 1.013 bar; Isentropic efficiency of GT: 0.92.
Air compressor for NH_3 cases	Isentropic efficiency: 0.85.
Solar heat supply process	DNI: 1022 W/m^2 [43]; Collector efficiency: 0.568 [44].

3. System evaluation methodology

3.1 Energy analysis

For energy analysis, power generation efficiency and energy penalty are the key indicators for system evaluation. The detailed calculation of power generation efficiency is shown Eq. (1).

$$\eta_p = \frac{P_{GT} + P_{STs} - P_{Pumps} - P_{ASU} - P_{Comps}}{m_{NG} LHV_{NG} + m_{NH_3} LHV_{NH_3} + Q_{solar,receive}} \quad (1)$$

Here, the numerator represents the system's power output, while the denominator indicates the system's energy input. P_{GT}, P_{STs}, P_{Pumps}, P_{ASU}, and P_{Comps} represent the power generation in gas turbines and steam turbines, and power consumption in pumps, ASU unit and compressors, respectively. Besides, m_{NG}, and m_{NH3} represent mass flow of natural gas input and NH_3 input in these systems, respectively. LHV_{NG}, and LHV_{NH3} are the lower heating value of natural gas input and NH_3 input, respectively. $Q_{\text{solar,receive}}$ is the heat received by the solar field.

P_{GT} and P_{STs} denote the power generated by the gas turbine and steam turbines, respectively, while

P_{Pumps}, P_{ASU}, and P_{Comps} represent the power consumed by the pumps, air separation unit (ASU), and compressors, respectively. Additionally, m_{NG}, and m_{NH3} signify the mass flow rates of natural gas and ammonia inputs into the system, respectively. The terms LHV_{NG}, and LHV_{NH3} refer to the lower heating values of natural gas and ammonia, respectively. Finally, $Q_{\text{solar,receive}}$ represents the thermal energy absorbed by the solar field.

The energy penalty refers to the decrease in power generation efficiency of a power plant after adding a CO_2 capture unit. The energy penalty is defined in Eq. (2) [45].

$$\Delta\eta = \eta_{p,w} - \eta_{p,wo} \tag{2}$$

Where $\eta_{\text{p,w}}$ and $\eta_{\text{p,wo}}$ are the power generation efficiencies of the NGCC power plants with and without CO_2 capture, respectively.

The CO_2 capture rate (CCR) is the ratio of CO_2 captured to the total carbon entering the system. In a calcium looping carbon capture system, carbon comes from two sources: the flue gas and the fuel used to supply energy for the calcination process. It can be calculated using the following equation:

$$CCR = \frac{n_{\text{CO2,captured}}}{n_{\text{CO2,f}} + n_{\text{C,esf}}} \tag{3}$$

where $n_{\text{CO2,captured}}$ represents the amount of CO_2 captured, and $n_{\text{CO2,f}}$ is the amount of CO_2 in the flue gas entered the carbonator, and $n_{\text{C,esf}}$ represents the carbon content in the energy supply fuel for calcination process. Specifically, $n_{\text{C,esf}}$ in the CaL-OXY system represents the carbon content in the natural gas input for the calcination process. For the CaL-NH_3 and CaL-SOL systems, since there is no additional input of carbon-containing fuel, $n_{\text{C,esf}}$ is 0, and the captured CO_2 only comes from the flue gas of the power plant.

Primary energy saving ratio (*PESR*) is a key indicator assess the system performance based on the primary energy consumption under the same work output as the reference system. Considering that the ammonia is the secondary energy, the ammonia sources should be considered in this calculation. For the CaL-NH_3 system, CaL-OXY and primary energy to ammonia to power systems (PE-NH_3-P) can be selected as the reference systems. *PESR* can be calculated using the following formula:

$$PESR = \frac{P_{\text{ref1}} / \eta_{\text{P,ref1}} + P_{\text{ref2}} / \eta_{\text{P,ref2}} - P / \eta_{\text{P}}}{P_{\text{ref1}} / \eta_{\text{P,ref1}} + P_{\text{ref2}} / \eta_{\text{P,ref2}}} \tag{4}$$

where ref1 and ref2 represent the CaL-OXY system and primary energy to ammonia to power

system, respectively.

3.2 Life cycle assessment

Life Cycle Assessment (LCA) is a method used to evaluate the environmental effects of a product, process, or service over its entire life. This includes all stages, from getting raw materials, making the product, using it, and finally disposing or recycling it. The LCA process has four main steps: defining goals and scope, analyzing the inventory, assessing impacts, and interpreting results. In this study, a process-based LCA was used to evaluate the environmental impacts of NGCC power plants with CO_2 capture over their full life cycle.

3.2.1 Life cycle assessment indicators

In this study, a process-based LCA was conducted to comprehensively evaluate the environmental impacts associated with various products across their entire life cycle. The assessment incorporated several key indicators, each representing distinct aspects of environmental impact. Global Warming Potential (GWP) and Primary Energy Demand (PED) were utilized to analyze the system's contribution to climate change and overall energy consumption. These indicators are essential for understanding the broader implications of greenhouse gas emissions and the energy required throughout the life cycle, from resource extraction to end-of-life disposal. Water Use (WU) was included to measure the total volume of freshwater consumed, highlighting the importance of sustainable water management, especially in regions facing water scarcity. And Acidification Potential (AP) and Eutrophication Potential (EP) were adopted to evaluate the impact of acidifying substances and nutrient emissions on ecosystems. Furthermore, Respiratory Inorganics (RI) and Photochemical Ozone Formation Potential (POFP) were analyzed to assess the health impacts related to air quality, with RI highlighting the respiratory issues caused by particulate matter and inorganic pollutants, while POFP evaluates the formation of ground-level ozone, a key smog component that exacerbates respiratory problems. Finally, Human Toxicity (HT) and Ecotoxicity (ET) were also considered to evaluate the potential harmful effects of substances on human health and ecosystems. Table 2 displays the indicators and the corresponding unit used in this study.

Table 2 Life cycle assessment indicators

Indicator	Abbreviation	Unit

Global Warming Potential	GWP	kg CO_2-eq
Primary Energy Demand	PED	MJ
Water Use	WU	kg
Acidification Potential	AP	kg SO_2-eq
Eutrophication Potential	EP	kg PO_4-eq
Respiratory Inorganics	RI	kg PM2.5-eq
Photochemical Ozone Formation Potential	POFP	kg NMVOC-eq
Potential Ecotoxicity	ET	CTU_e
Human toxicity	HT	CTU_h

3.2.2 Functional unit (FU) and system boundary

The functional unit acts as a benchmark that links all inputs and outputs in the analysis. In this study, the functional unit was defined as one kWh of net electricity produced and delivered, which is a common standard for power plant assessments. Furthermore, since the system exclusively generates electricity, there are no allocation challenges to address. Fig.6 shows the system boundary of NGCC power plants with CCS, covering upstream processes (e.g., natural gas production and transportation, material and energy supply, and infrastructure construction), power generation, flue gas purification and decarbonization, CO_2 transport and sequestration, the downstream processes of waste disposal and plant decommission.

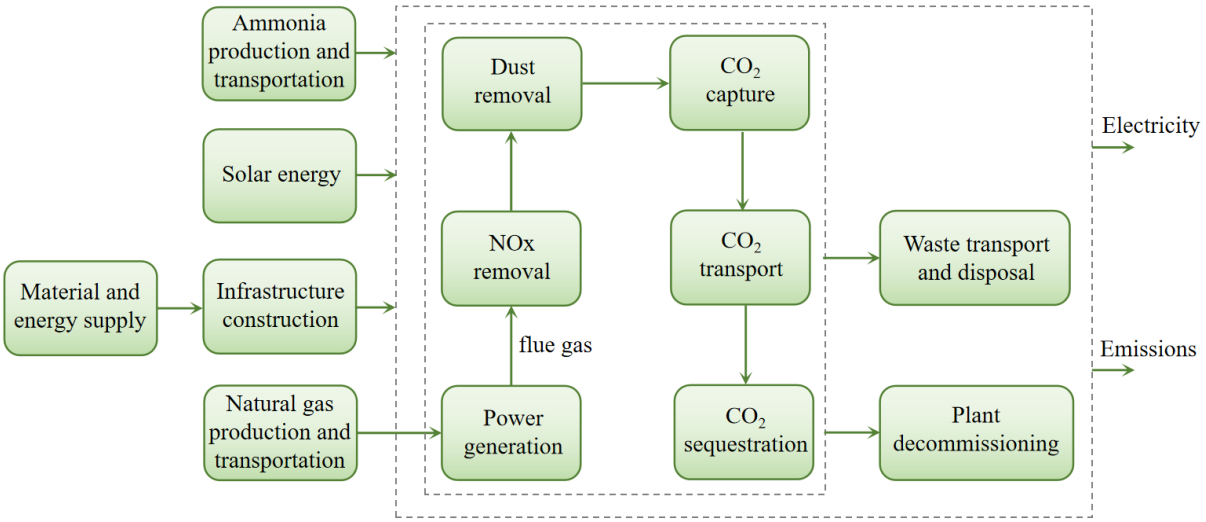

Fig.6 System boundary of NGCC power plants with CCS

3.2.3 Inventory data

The software used in this study is an online LCA tool called eFootprint. It uses data from the CLCD (2020), Ecoinvent (2020), and ELCD (2020) databases. China was chosen as the location for the LCA. The NGCC power plant in this study is in Dongguan, Guangdong Province. Most of the background data came from the CLCD-China-ECER 0.8 database, which reflects the average technology level in the Chinese market. Table 3 lists the main data sources used for the LCA.

Table 3 Main data sources for LCA

No.	Item	Source
1	Background data for material production parameters for PCC power plants	CLCD, Ecoinvent V3.1
2	Operation parameters for PCC power plants	Simulation results from Aspen Plus
3	Inventory data for power plant construction	Scientific publications [46-48]
4	Inventory data for natural gas extraction and transportation	Ecoinvent V3.1
5	Inventory data for ammonia production	Scientific publications [49]
6	Inventory data for CO_2 transportation and storage	Ecoinvent V3.1

3.2.4 CO_2 transport and storage

The life cycle assessment must also consider how the captured CO_2 is stored. The captured CO_2 is moved through pipelines at a starting pressure of 110 bar, traveling 200 km, with a leakage rate of about 0.026% per 1000 km [50]. For storage, saline aquifers are used, as they are expected to have the largest storage capacity for CO_2 in China. This study does not look at issues like storage leaks or decommissioning. The storage site is assumed to be about 1500 meters deep, and the energy needed to inject CO_2 is estimated at 6.5 kWh per ton of CO_2 [51].

3.3 Life cycle cost assessment

In addition to considering environmental impacts, the life cycle economic assessment can evaluate the economic feasibility of various CCUS technology pathways. The Levelized Cost of Energy (*LCOE*) for carbon capture power plants measures the average cost per unit of electricity

generated, accounting for all capital, operational, and carbon capture-related expenses over the plant's lifetime, which can be calculated by Eq. (5):

$$LCOE = \frac{CRF \times CAPEX + X_{OM} \times CAPEX + C_{FUEL}}{CF \times T \times P_{net}} \tag{5}$$

where the first item of numerator represents the annual investment cost, and the second and the third item of numerator represent the annual operating & maintenance (O&M) cost and annual fuel cost, respectively. *CF* is the capacity factor of system and *T* indicates the annual operation hours (hours/year).

As is shown in the Eq. (5), the annual investment cost is calculated by the total capital expenditure (*CAPEX*) and the capital recovery factor (*CRF*). The *CAPEX* consists of direct plant cost (DPC), indirect plant cost (IPC), Contingency, Contractor fee, and working capital (WC), which is highly related to the capital cost of each component. While the *CRF* is related to the discounted rate and the life of equipment, The *CRF* can be calculated by the Eq. (6).

$$CRF = \frac{i \times (i+1)^n}{(i+1)^n - 1} \tag{6}$$

where *i* and *n* represent the discounted rate and the equipment operating life, respectively.

The capital cost of each component is empirically estimated by means of scaling factor exponent, which is shown as Eq. (7):

$$I_i = \frac{CEPCI_{2023}}{CEPCI_{ref}} I_{i,r} \left(\frac{S_i}{S_{i,r}}\right)^{f_i} \tag{7}$$

where I_i represents the cost of the equipment at the actual scale, and $I_{i,r}$ represents the cost of the equipment at the reference scale. Since the reference scale and economic data are based on previous years, all economic data have been adjusted according to the Chemical Engineering Plant Cost Index (CEPCI). *S* represents the scale of the equipment, with the subscripts *i*, *r* and the variable *f* denoting the *i*-th equipment, the reference equipment, and the scaling factor, respectively. More detailed calculation parameters of *CAPEX* can be found in Tables S9-S11 in the Supplementary document.

The cost of CO_2 removed (*COR*) is a key indicator to evaluate the economic performance of carbon capture power plants, which can be calculated as:

$$COR = \frac{LCOE_{cap} - LCOE_{ref}}{CO_{2,ref} - CO_{2,cap}} \tag{8}$$

where $LCOE_{cap}$ and $LCOE_{ref}$ are the levelized cost of energy for carbon capture power plants and the reference power plant without CO_2 capture, respectively; $CO_{2,ref}$ and $CO_{2,cap}$ are the direct CO_2 emission from reference power plants without CO_2 capture and carbon capture power plants, respectively.

When evaluating the life cycle of a system, the Life Cycle Cost (*LCC*) and greenhouse gas (GHG) emissions can be combined into a single metric called the Life Cycle Cost of GHG Removed (*LCOR*). This metric measures the cost required to achieve net reductions in GHG emissions over the entire life cycle, rather than simply focusing on the amount of CO_2 captured. The *LCOR* can be determined using Eq. (9):

$$LCOR = \frac{LCOE_{cap} - LCOE_{ref}}{GHG_{ref} - GHG_{cap}} \tag{9}$$

4. Results and Discussion

4.1 Energy analysis results

Based on the assumptions regarding the key operational parameters of the carbon capture system outlined in Section 3, Fig.7 presents the energy analysis results for the three carbon capture technology pathways. The results indicated that replacing fossil fuels with solar energy for heating lowers overall system efficiency, with a 4.5 percentage point increase in the energy penalty. This is mainly due to the lower solar-to-thermal conversion efficiency of 57.8%, leading to higher energy demand for CaL-SOL compared to CaL-OXY. Additionally, under the same 90% capture rate, CaL-OXY benefits from reduced CO_2 absorption in the carbonation tower due to the oxy-fuel combustion, which decreases the required mass flow of CaO and the heat demand for calcination.

On the other hand, the CaL-NH_3 method shows a notable improvement in system performance, with an energy penalty of only 2.6 percentage points. This lower energy penalty is mainly due to the integration of the calcium looping process with chemical energy conversion, which allows for more efficient recovery and conversion of chemical energy into power. In the CaL-NH_3 system, the chemical energy input to the CaL unit is 403.8 MW, leading to a power output increase of 186.3 MW. In comparison, the CaL-Oxy method achieves only a 42.4 MW increase in power output despite a chemical energy input of 187.2 MW, primarily because of inefficient heat recovery and the additional power consumed by the air separation unit (ASU). In the CaL-NH_3 approach, part of the heat from the carbonation reaction is recovered and converted into chemical energy stored in the cracked products.

This chemical energy is then transformed into high-grade thermal energy for the calcination process and further utilized for power generation through the combined cycle. In contrast, the CaL-Oxy method relies on direct combustion to convert chemical energy into heat for calcination, with high-grade thermal energy recovered through the Rankine cycle in the HRSG unit. By efficiently utilizing NH_3 in the combined cycle, the proposed system not only enhances power generation but also eliminates the need for ASU power consumption, resulting in a significantly lower energy penalty.

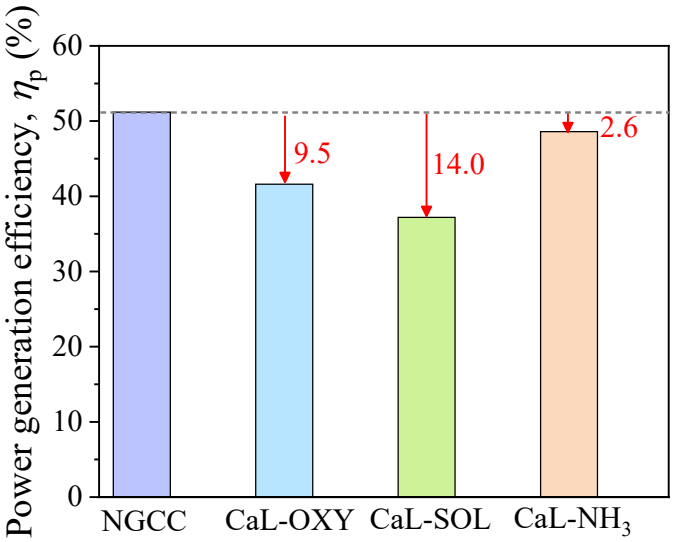

Fig.7 Power generation efficiency of various carbon capture pathways

Given that the source of ammonia influences the primary energy saving ratio of ammonia-driven carbon capture technology pathways, Fig.8 shows the impact of ammonia sources on *PESR*. The ammonia sources considered include hydrogen produced from PV, wind-powered electrolysis, biomass gasification, coal gasification, and coal gasification with CCS. From the results in Fig.8, the CaL-NH_3 systems exhibit a primary energy saving ratio of 18~19%. This indicates that the new system demonstrates a favorable primary energy saving ratio regardless of the ammonia source. However, due to the lower efficiency of photovoltaic power generation, the NH_3-PV system has the lowest *PESR* at 18.2%. But, overall, the impact of the ammonia source on *PESR* is minimal.

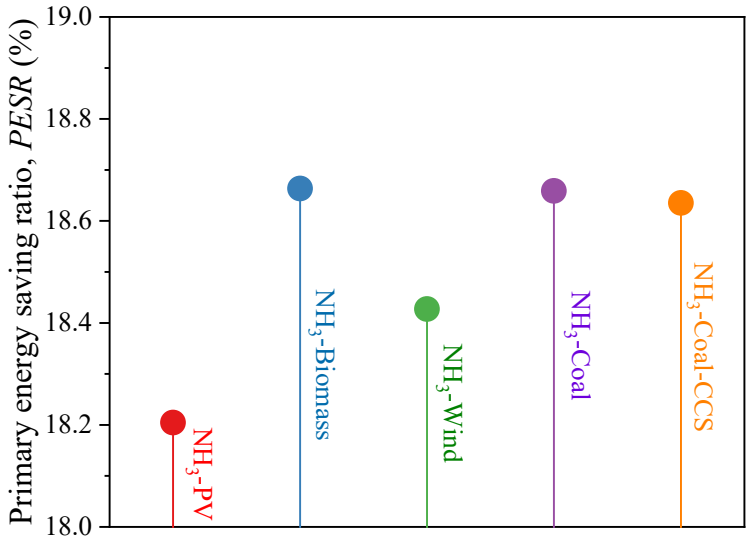

Fig.8 Primary energy saving ratio under different ammonia sources

4.2 Life cycle assessment results

4.2.1 Comparison between various technical routes

Based on the results of the energy analysis in Section 4.1 and the research on material consumption for infrastructure construction found in the literature, the Life Cycle Inventory (LCI) for NGCC and NGCC-PCC systems can be determined. The LCI data list includes materials and fuel consumption for construction, materials and fuel consumption for operation, emissions during operation, and fuel consumption for plant decommissioning. The LCI for NGCC power plants and NGCC-PCCs can be found in Table S3 in the Supplementary Document. By inputting the LCI data into the eFootprint online software, it is possible to calculate the life cycle assessment results for each technological pathway.

Fig.9 presents the life cycle assessment results for NGCC, CaL-OXY, CaL-SOL and CaL-NH_3. Due to differences in the units and scales of these indicators, Fig.9 normalizes the data to facilitate comparison between the different technologies. Each indicator is normalized by setting the maximum value among the four technologies to 1, with the values for the other technologies represented as a ratio of the actual value to the maximum value. The specific numerical values are also listed in Table 5.

Fig.9 demonstrates that all the three CaL pathways achieve a substantial reduction in GWP compared to NGCC power plants. Among these, CaL-SOL has the lowest GWP (170.7 g CO_2-eq/kWh), representing approximately 35% of that in an NGCC plant without capture (476.9 g CO_2-eq/kWh).

And the CaL-OXY pathway follows, with a GWP close to 45% of that in NGCC power plants, at 207.7 g CO_2-eq/kWh. This reduction is primarily due to the additional CO_2 emissions and increased natural gas consumption required for the calcination process. CaL-NH_3 shows a higher GWP of 258.8 g CO_2-eq/kWh compared to the other two CaL technologies. This elevated GWP is largely due to the relatively high carbon emissions associated with ammonia production, especially when using the well-established photovoltaic electrolysis for ammonia synthesis.

As for Primary Energy Depletion (PED), CaL-OXY records the highest value at 9.54 MJ, considerably higher than that of NGCC, while CaL-SOL shows a modest reduction. In contrast, CaL-NH_3 demonstrates a significant decrease, with PED dropping to 4.16 MJ. This is primarily due to the fact that CaL-OXY relies on natural gas to provide heat for the calcination process, leading to higher primary energy consumption compared to other pathways. Meanwhile, CaL-NH_3 uses ammonia as the energy source, which not only reduces natural gas consumption but also significantly increases the life cycle electricity output of the carbon capture plant, thereby substantially lowering the primary energy consumption per unit of electricity generated.

The Water Intensity (WU) of the system is primarily influenced by the water consumption of the steam Rankine cycle and the total electricity generation over the system's lifecycle. Among all the technological pathways, CaL-OXY exhibits the highest WU, followed by CaL-SOL, with NGCC having the lowest. Clearly, the introduction of CaL technology reduces the lifetime output of the power plant, increasing the unit water consumption for power generation, and exacerbates efficiency penalties, leading to a more pronounced increase in WU. As highlighted in energy analysis in Section 2.3, CaL-OXY faces the highest energy penalty at 9.5 points, whereas CaL-NH_3 has the lowest penalty at 2.6 points. Consequently, WU significantly increases for CaL-OXY, while the increase for CaL-NH_3 is relatively minor.

Acidification Potential (AP) and Eutrophication Potential (EP) reflect the system's potential for acidification and eutrophication, respectively. Among the various technological routes, CaL-NH_3 shows notably higher AP and EP values than the other options. This significant increase is primarily due to the ammonia production process. Specifically, the use of hydrogen production via photovoltaic electrolysis (PV) for ammonia synthesis involves materials and chemicals that can be harmful, as well as potential nitrogen oxide emissions. These factors contribute to the elevated AP and EP values for CaL-NH_3. And for Ecotoxicity (ET) and Human Toxicity (HT), CaL-NH_3 also presents considerable

drawbacks compared to other technologies, largely due to the impacts associated with the PV-based ammonia production. Conversely, NGCC and CaL-OXY exhibit minimal ET and HT. CaL-SOL, while also having relatively low toxicity impacts, shows some ecological and human toxicity linked to the construction of solar thermal plants.

Besides, the introduction of the CaL technology results in an increase in both Respiratory Inorganics (RI) and Photochemical Ozone Formation Potential (POFP) compared to NGCC. The rise in RI across all three capture technology pathways is largely attributed to the significant dust and particulate matter generated during the production of $CaCO_3$ and disposal of CaO. Additionally, natural gas extraction and ammonia production processes emit VOCs and NOx, which participate in photochemical reactions under sunlight to form ground-level ozone, contributing to higher POFP values. For CaL-OXY and CaL-SOL, the increase in RI and POFP compared to NGCC is primarily due to the reduced lifetime power output of the system. In the case of CaL-NH_3, the increase in these indicators is also influenced by the ammonia production process, which exacerbates the emissions of VOCs and NOx.

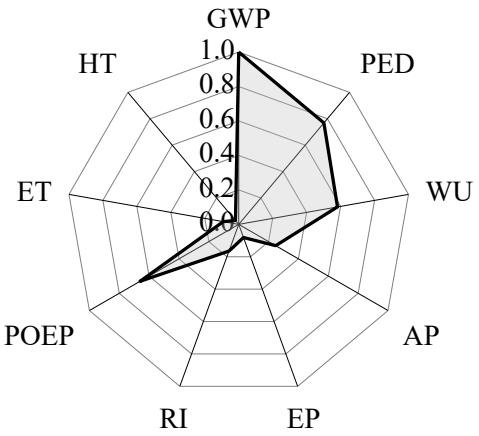

(a) NGCC

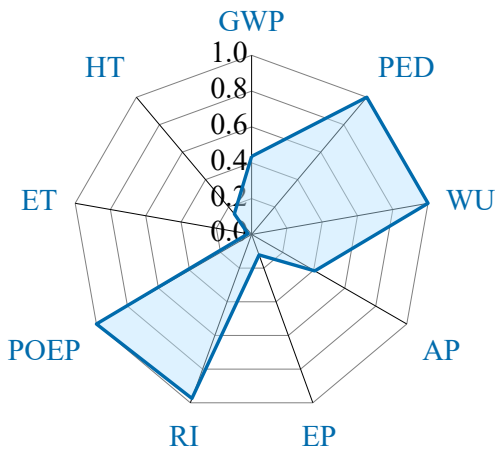

(b) CaL-OXY

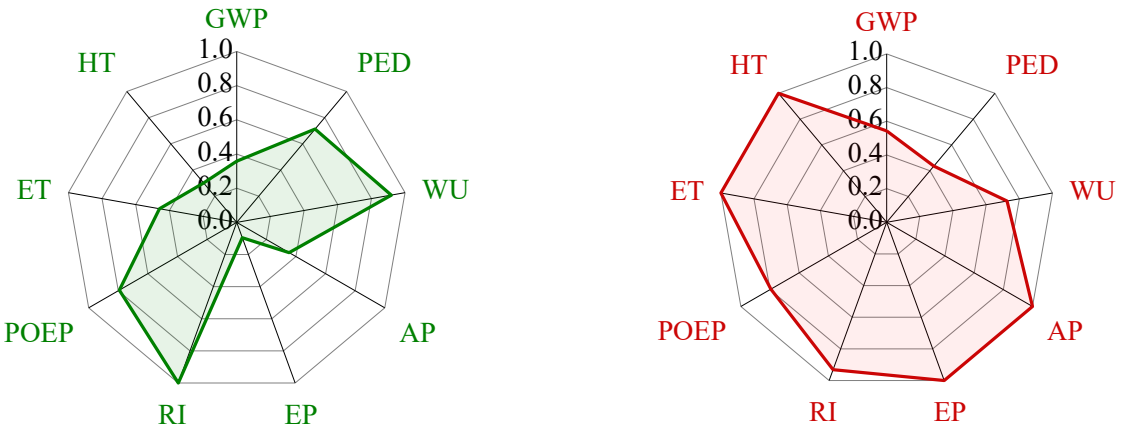

(c) CaL-SOL **(d) CaL-NH3**

Fig.9 Spider chart for LCA results comparison

Table 5 LCA results comparison of various CaL technologies

	NGCC	NGCC-CLC-OXY	NGCC-CLC-SOL	NGCC-CLC-NH_3
GWP (g CO_2-eq)	476.94	207.7	170.7	258.8
PED (MJ)	7.33	9.54	6.80	4.16
WU (kg)	1.74	3.12	2.87	2.27
AP (kg SO_2-eq)	3.92×10^{-4}	6.49×10^{-4}	5.64×10^{-4}	15.9×10^{-4}
EP (kg PO_4-eq))	6.78×10^{-5}	1.01×10^{-4}	7.97×10^{-5}	8.35×10^{-4}
RI (kg PM2.5-eq)	6.11×10^{-5}	3.66×10^{-4}	3.75×10^{-4}	3.50×10^{-4}
POEP (kg NMVOC-eq)	2.12×10^{-4}	3.22×10^{-4}	2.55×10^{-4}	2.55×10^{-4}
ET (CTUe)	0.09	0.02	0.45	0.98
HT (CTUh)	1.03×10^{-8}	5.20×10^{-8}	1.05×10^{-7}	3.48×10^{-7}

4.2.2 The impact of ammonia sources for the CaL-NH_3 system

Given that the source of ammonia significantly influences the LCA results of ammonia-driven carbon capture technology pathways, this section will explore the impact of ammonia sources on the life cycle performance of the CaL-NH_3 route. The ammonia sources considered is the same as Section 4.1. Some environmental impact data for different ammonia sources can be found in ref.[49]. The results are shown in Fig.10, where the value of NGCC power plants is chosen as the reference point (100%) and compares the relative environmental performance for each ammonia source.

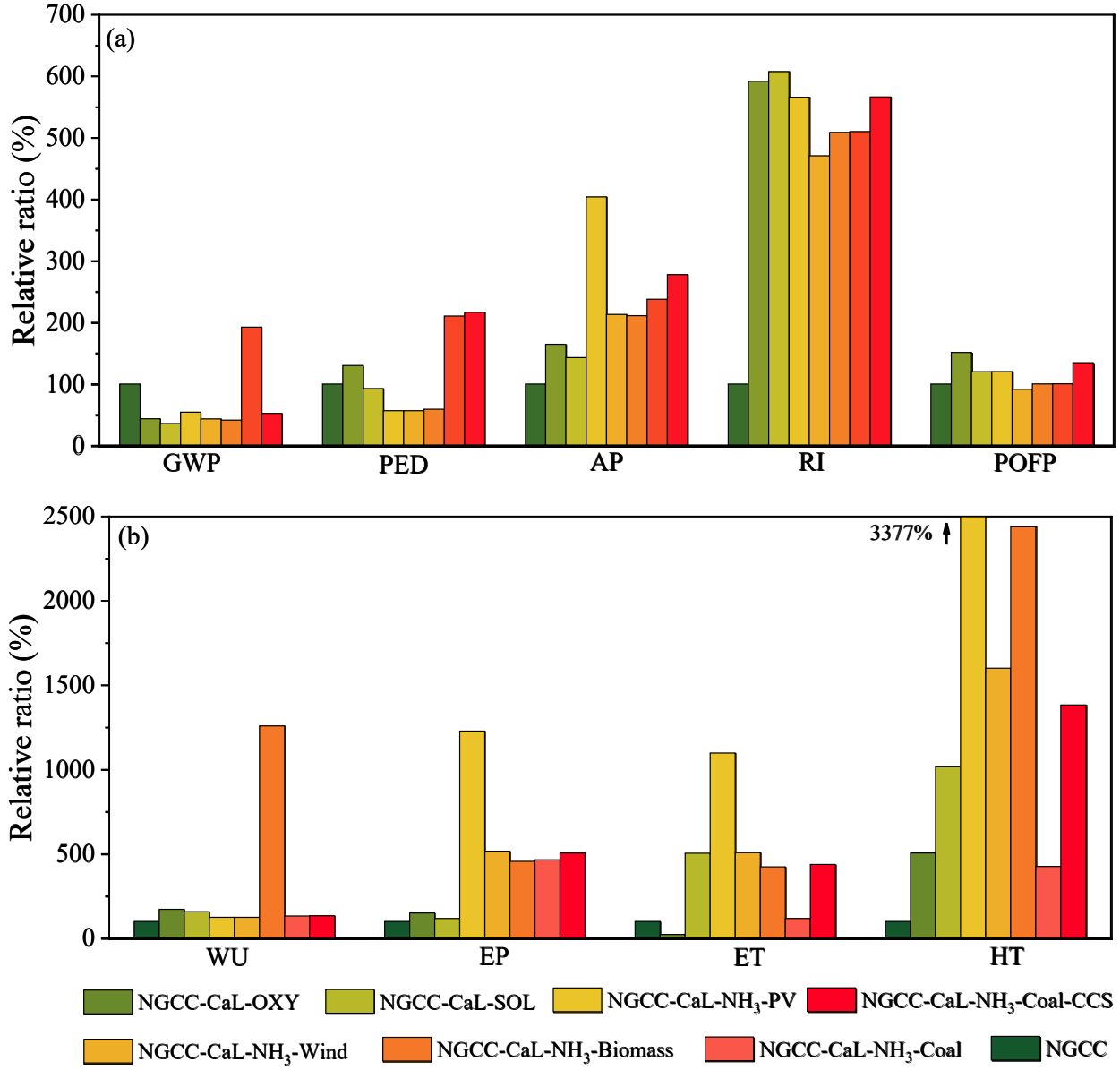

Fig.10 Sensitive analysis of NH_3 sources on CaL-NH_3 systems

The results indicate that different ammonia sources significantly impact the life cycle performance of the CaL-NH_3 technology route. For GWP, the introduction of the CaL technology generally leads to a notable reduction in GWP across most systems. Among these, CaL-SOL has the lowest GWP at 170.7 g CO_2-eq/kWh, due to the use of solar heat. In contrast, CaL-OXY, which relies on fossil fuels, has a higher GWP of 207.7 g CO_2-eq/kWh compared to the solar-driven case. In ammonia-driven systems, if ammonia is derived from coal gasification (gray ammonia), the GWP is the highest at 917.9 g CO_2-eq/kWh, significantly exceeding that for NGCC power plants at 476.9 g CO_2-eq/kWh. However, if CCS is added to the coal gasification process, the GWP for blue ammonia drops to 249.5 g CO_2-eq/kWh. Furthermore, ammonia produced from renewable energy sources, such

as PV, wind, and biomass, maintains relatively low GWP values. Among these, biomass gasification has the lowest GWP at 197.6 g CO_2-eq/kWh, though this is still ~15% higher than that for CaL-SOL. And the GWPs for PV and wind-powered ammonia production are 258.8 g CO_2-eq/kWh and 207.1 g CO_2-eq/kWh, respectively.

PED and WU are closely related to primary energy consumption and water consumption. Among the various ammonia production routes, coal-based ammonia production has the highest PED due to the high energy density of coal, low conversion efficiency, and substantial energy consumption. In contrast, other ammonia production methods exhibit a significant reduction in PED compared to coal-based cases. Regarding water resources, the adoption of the CaL technology generally increases water consumption at power plants. Specifically, CaL-NH_3 with biomass gasification for ammonia production has a significantly higher WU compared to other technologies. This is primarily due to the substantial water consumption associated during the biomass collection process, accounting for 99% of the total water use throughout the biomass-to-hydrogen life cycle [52].

In terms of AP and EP, the CaL-NH_3 method exhibits significantly higher impacts than CaL-OXY and CaL-SOL methods, particularly when ammonia is produced via PV electrolysis. This is primarily due to the material extraction, energy consumption, and chemical use involved in manufacturing PV panels, which releases acidifying gases and water pollutants. Similarly, wind-powered electrolysis for ammonia production also contributes to AP and EP due to emissions from the manufacturing of turbines and electrolyzers. Besides, biomass and coal gasification routes, including those using CCS, further increase AP and EP due to emissions from gasification and chemical usage.

Regarding RI, systems employing CaL technologies for CO_2 capture exhibit significantly higher impacts than NGCC plants. This is primarily due to particulate emissions during $CaCO_3$ production and CaO disposal processes. Ammonia-based systems powered by renewable sources, particularly those using wind and biomass, show relatively lower RI due to their cleaner production processes. However, coal gasification produces higher levels of SO_x, NO_x, and particulates, contributing to elevated RI. Although PV-ammonia systems are relatively clean during operation, the production of PV panels involves substantial emissions that increase RI.

As for ET and HT, the CaL-NH_3 method, especially with PV ammonia production, has the highest ET and HT due to the materials and chemicals used in manufacturing PV panels. Similarly, the CaL-NH_3 method with wind-based ammonia, and coal gasification with CCS also show elevated toxicity,

attributed to heavy metal usage and toxic chemicals during the production and chemical absorption processes. Besides, biomass gasification leads to higher ET and HT compared to coal gasification, largely due to the complexity of biomass feedstocks and the challenges in controlling harmful byproducts during gasification.

4.2.3 Contribution analysis for various environment impacts

The previous section compared the various environmental indicators of different carbon capture technical routes, and this section will further analyzed the contribution of various sub-processed on the environmental indicators. The CaL systems is divided into 11 sub-processes, including plant infrastructure, natural gas production and transportation, ammonia production and transportation, $CaCO_3$ and water supplies, other supplies, direct emissions, CO_2 transport and storage, and plant waste treatment processes. Plant infrastructure includes the construction of the power plant and capture unit, while natural gas production refers to the extraction and purification of natural gas. Natural gas transportation includes the shipping and pipeline transport of liquefied natural gas. Ammonia production involves the different ammonia generation methods discussed earlier, and ammonia transportation refers to the transportation of ammonia in trucks. $CaCO_3$ supplies cover the extraction and transportation of $CaCO_3$, and water supplies include the production and transportation of water. Other supplies refer to all materials and energy supplies except $CaCO_3$ and water, such as catalysts. Direct emissions account for emissions during power plant operation, while CO_2 transport and storage cover the construction and energy usage in pipelines and storage wells, including CO_2 transport and storage processes. Plant waste treatment considers the CaO treatment, waste disposal during plant decommissioning and associated energy consumption.

The results are demonstrated in Fig.11. It is evident that for NGCC plants, over 80% of GWP is caused by direct CO_2 emissions, while the rest stems from natural gas production and transportation. PED, AP, EP, RI, and POEP are also largely driven by the natural gas production process, while WU mostly attributable to the operation of power plants. The plant construction, which involves heavy metals and chemicals, significantly contributes to ET and HT.

For the CaL-OXY and CaL-SOL methods, the contribution of each sub-processes to the indicators is similar, except for ET and HT. This difference is mainly due to the impact of the construction of solar collector fields, which has a greater impact on ET and HT. For the CaL-OXY method, in addition to the construction of carbon capture power plants, the construction of CO_2 transportation pipelines

and storage wells also has notable contributions. Unlike NGCC, the direct CO_2 emissions of the CaL-OXY method and the CaL-SOL method are significantly reduced, shifting GWP impacts primarily to natural gas production and transportation. Besides, CO_2 transportation and storage, $CaCO_3$ supplies and plant waste treatment also made a contribution to AP, EP and POEP, while plant waste treatment (CaO treatment) made a significant contribution to RI.

In the CaL-NH_3 system, ammonia production heavily influences all indicators. For GWP, ammonia production contributes over 50% of emissions, with the lowest impact from biomass gasification (47%) and the highest from coal gasification (89%). In green ammonia pathways, natural gas production and transport account for over 90% of PED, while for grey and blue ammonia, coal consumption in ammonia production drives more than 70% of primary energy demand. In WU, ammonia production adds significant water use, with biomass gasification showing 91% of WU due to water-intensive biomass collection. Ammonia production also significantly impacts AP, EP, RI, and POEP, with little variation across ammonia sources. In terms of toxicity, coal gasification has minimal impact on ET and HT, while other ammonia pathways contribute heavily to both ET (>70%) and HT (around 50%).

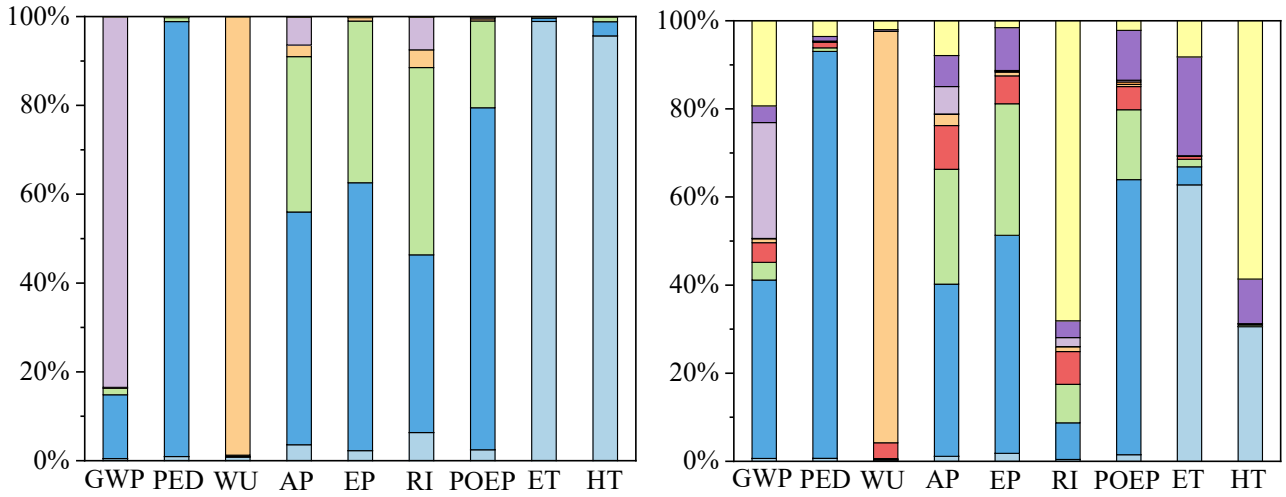

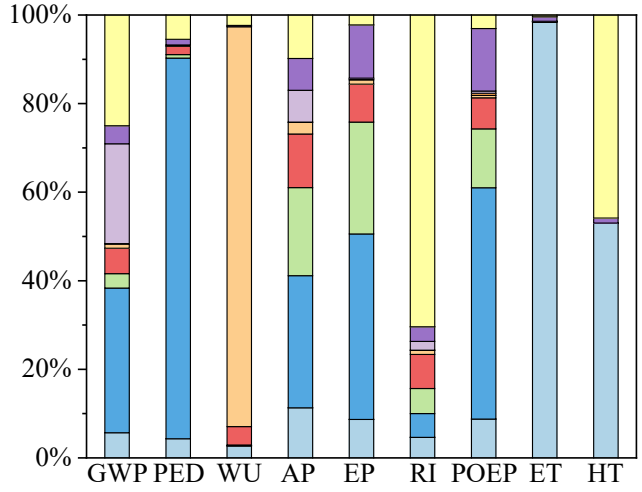

(c) NGCC-CaL-SOL

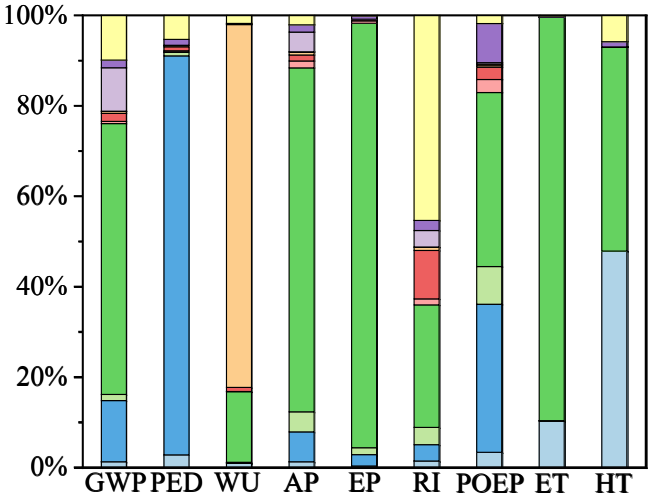

(d) NGCC-CaL-NH_3-PV

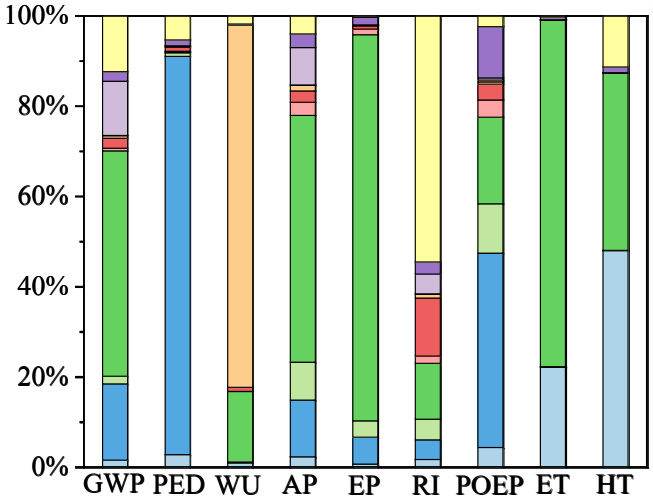

(e) NGCC-CaL-NH_3-Wind

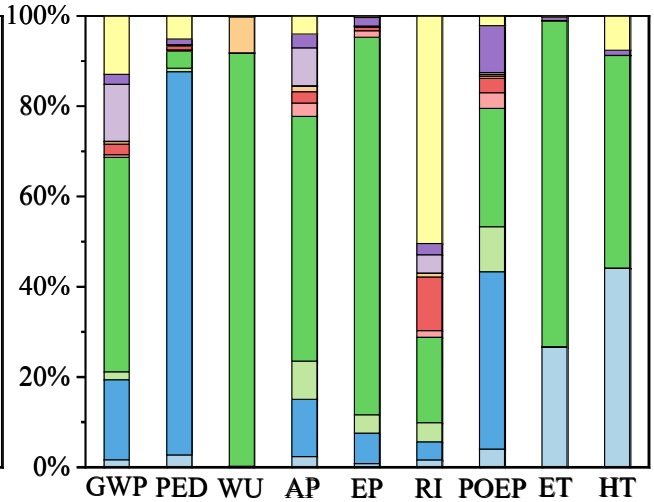

(f) NGCC-CaL-NH_3-Biomass

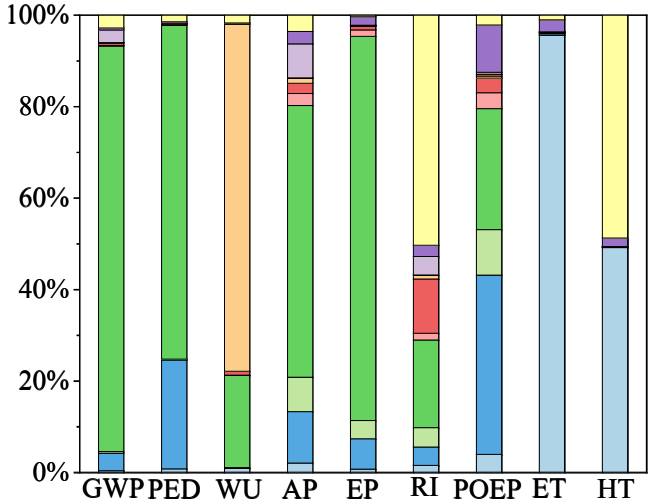

(g) NGCC-CaL-NH_3-Coal

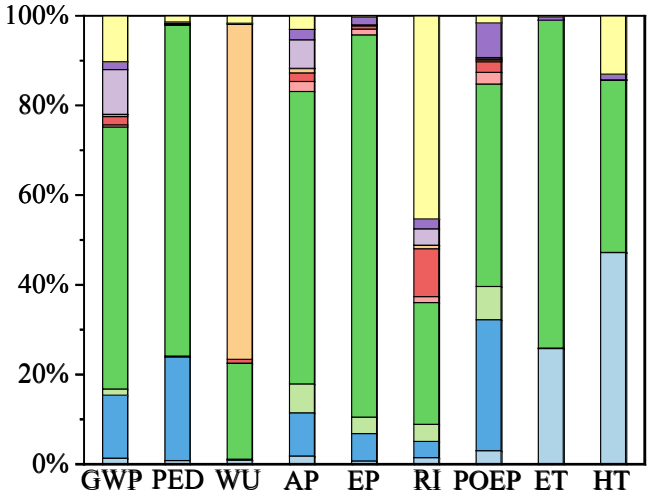

(h) NGCC-CaL-NH_3-Coal-CCS

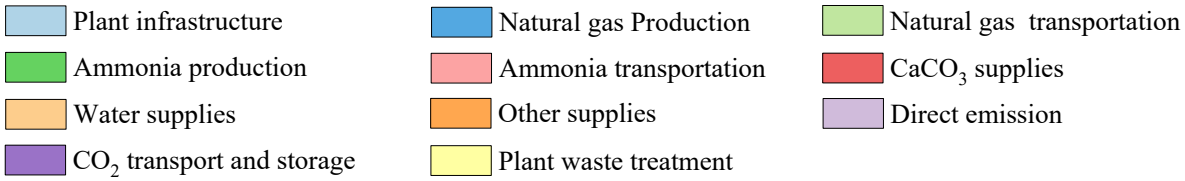

Fig.11 Contribution analysis of various technologies

4.2.4 Carbon footprint

In the previous sections, the impact of various technological pathways on different environmental indicators was comprehensively discussed. As GWP is a crucial indicator in environmental impact assessment, this section will provide a more detailed analysis of carbon footprint in each sub-processes. The aim is to trace the carbon footprint of the system and create a carbon footprint map to identify key areas for emission reduction. This analysis will offer guidance for the development of low-carbon systems.

Fig.12-15 illustrate the carbon footprints of the NGCC, CaL-OXY, CaL-SOL, and CaL-NH_3-PV systems. As shown in the figures, for the NGCC system, the majority of carbon emissions originate from the power plant flue gas, accounting for 83.5% of the total emissions, followed by natural gas extraction and purification processes, which contribute 14.4%. Emissions from other sub-processes, such as power plant construction, decommissioning, water supplies, and natural gas transportation, are relatively minor.

In contrast, the integration of calcium looping capture technology into the power plant leads to significant changes in the carbon footprint distribution. For example, in the CaL-OXY system, direct carbon emissions from the power plant flue gas are significantly reduced to 26.3% of the total emissions. The majority of emissions now come from natural gas production and transportation and CaO treatment, with negligible contributions from plant infrastructure and $CaCO_3$ production.

The carbon footprint distribution of the CaL-SOL system shows a similar overall trend to that of the CaL-OXY system. However, due to the shift from oxygen-enriched combustion heating to solar thermal heating in the calciner, natural gas consumption is reduced, leading to lower emissions from natural gas production and transportation. Additionally, with a 90% capture rate, the CaL-SOL system also sees a reduction in direct flue gas emissions. However, the construction of the solar heat collection field significantly increases the carbon footprint during the capture unit construction phase.

When ammonia-driven calcium looping capture is adopted, replacing natural gas with ammonia

for oxygen-enriched combustion significantly reduces emissions from natural gas production and transportation. Nonetheless, the primary source of emissions for the entire system shifts to ammonia production, which accounts for 59.9% of the total emissions, diminishing the impact of power plant flue gas on the overall carbon footprint. According to literature predictions [53], with cleaner production of photovoltaic panels, the carbon intensity of photovoltaic power generation is expected to decrease by nearly 30% by 2050, further reducing the carbon footprint of the CaL-NH_3-PV method.

Based on the analysis of carbon footprint in this study, the influence of different integration methods of tail-end and hot-end on GWP is further discussed. For the CaL-OXY system, GWP predominantly arise from natural gas production and transportation, direct emissions and CaO treatment. Under identical CO_2 capture rates and CaO conversion ratio, different integration methods require equivalent CaO processing capacities, rendering negligible influence on GWP. A comparative analysis [32] reveals that the hot-end integration strategy reduces direct CO_2 emission intensity by 12% (25.8 vs. 29.1 gCO_2/kWh) and natural gas consumption by 7.7% (0.60 vs. 0.65 kW/kWh), resulting in a reduced GWP relative to the tail-end strategy—a trend also observed in the CaL-SOL system. In the case of the CaL-NH_3 system, GWP extends beyond direct emissions and natural gas production and transportation processes to include NH_3 production and transportation processes. Based on our previous research on the hot-end integration method [54], by comparison, it can be known that the hot-end method demonstrates advantages in direct emission intensity (18.6 vs. 21.1 g/kWh) and natural gas consumption (0.85 vs. 0.96 kW/kWh), the tail-end approach requires less NH_3 per unit of electricity (1.06 vs. 1.13 kW/kWh). Overall, while the hot-end integration approach demonstrates potential for lower GWP, the tail-end strategy exhibits reduced NH_3 consumption per unit of electricity. Since NH_3 production pathways significantly influence emissions from NH_3 synthesis and transportation, the tail-end method may paradoxically achieve GWP when utilizing high-emission NH_3 production methods such as coal-based synthesis, despite its higher operational emissions.

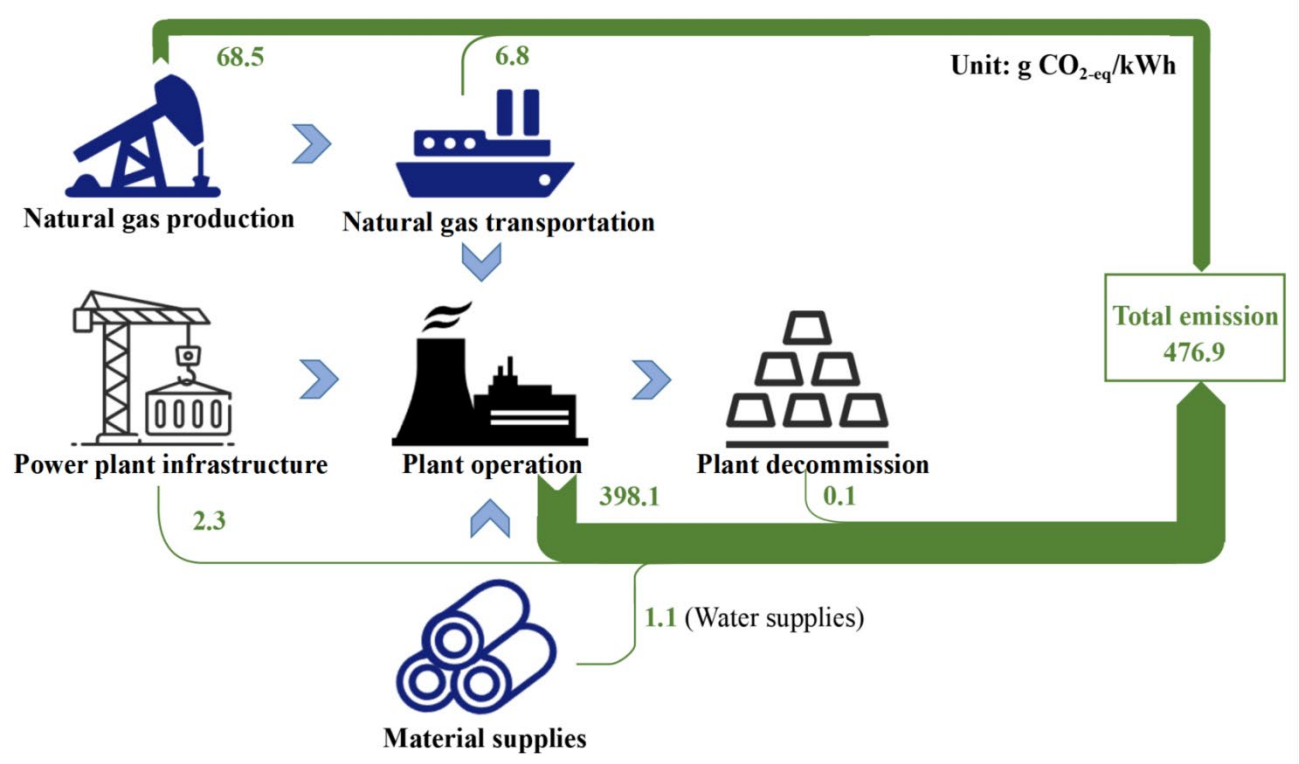

Fig.12 Carbon footprint of NGCC

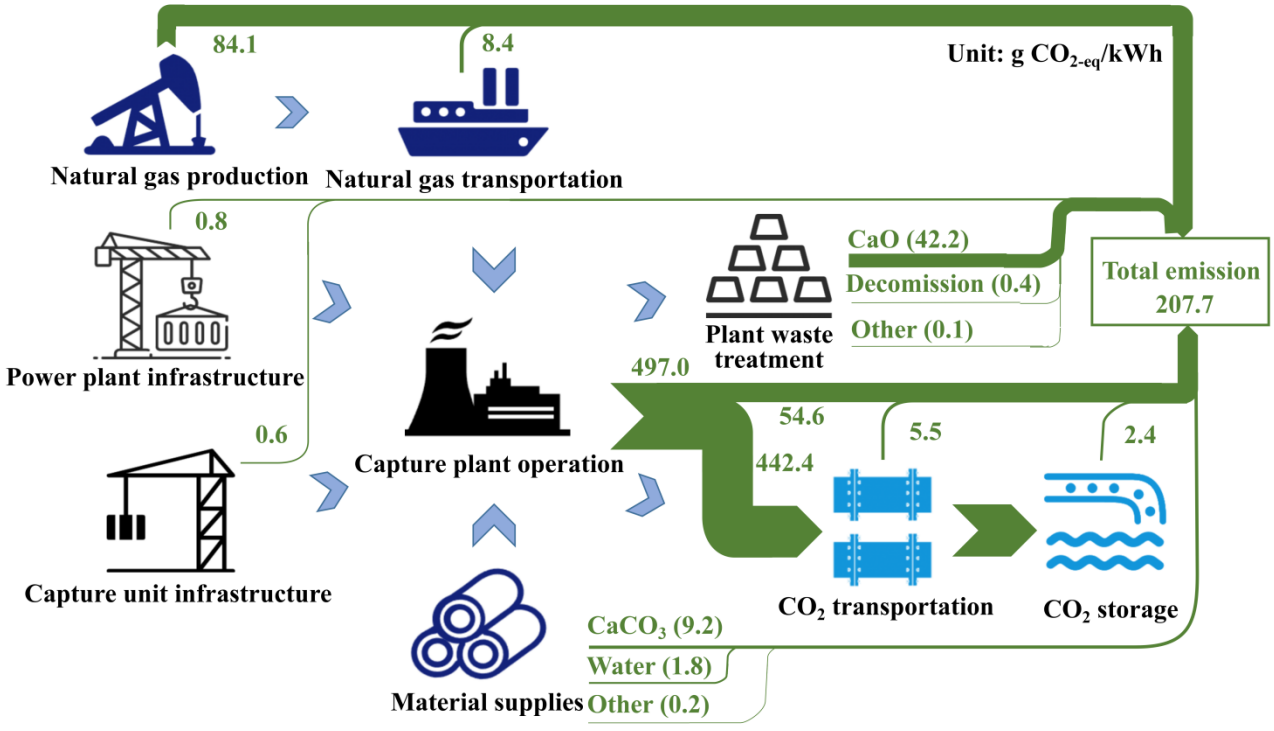

Fig.13 Carbon footprint of the CaL-OXY system

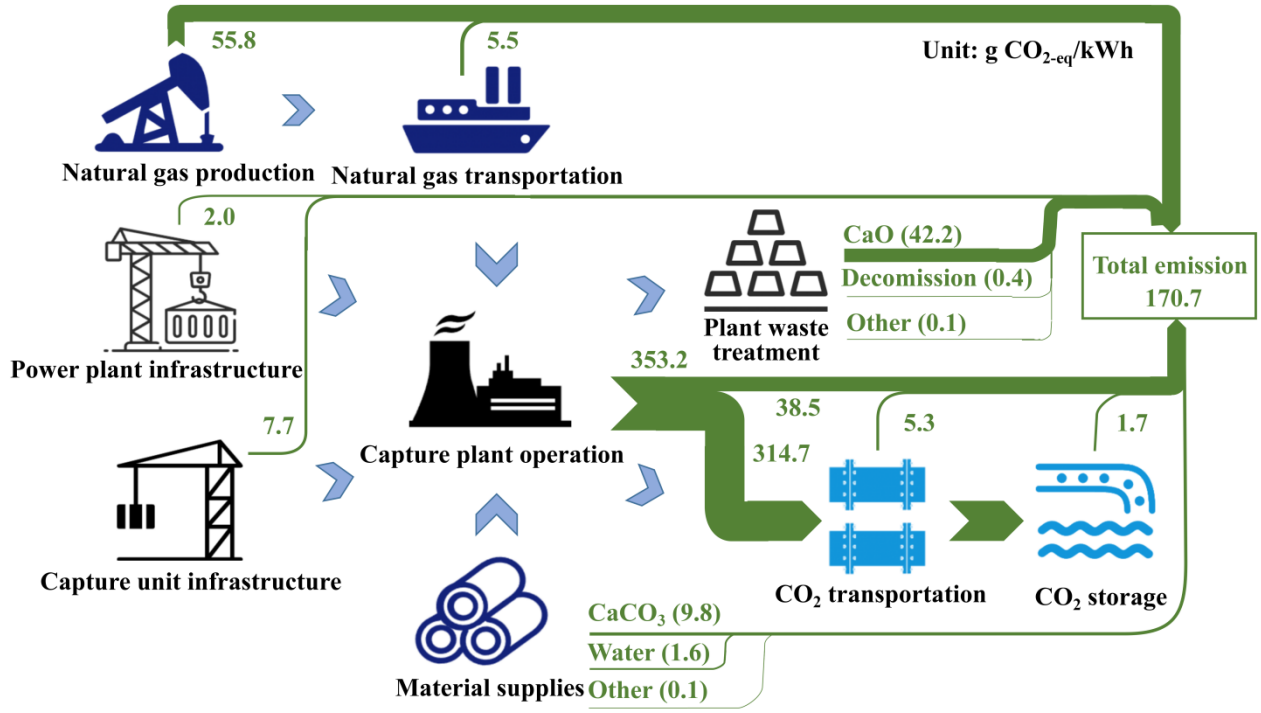

Fig.14 Carbon footprint of the CaL-SOL system

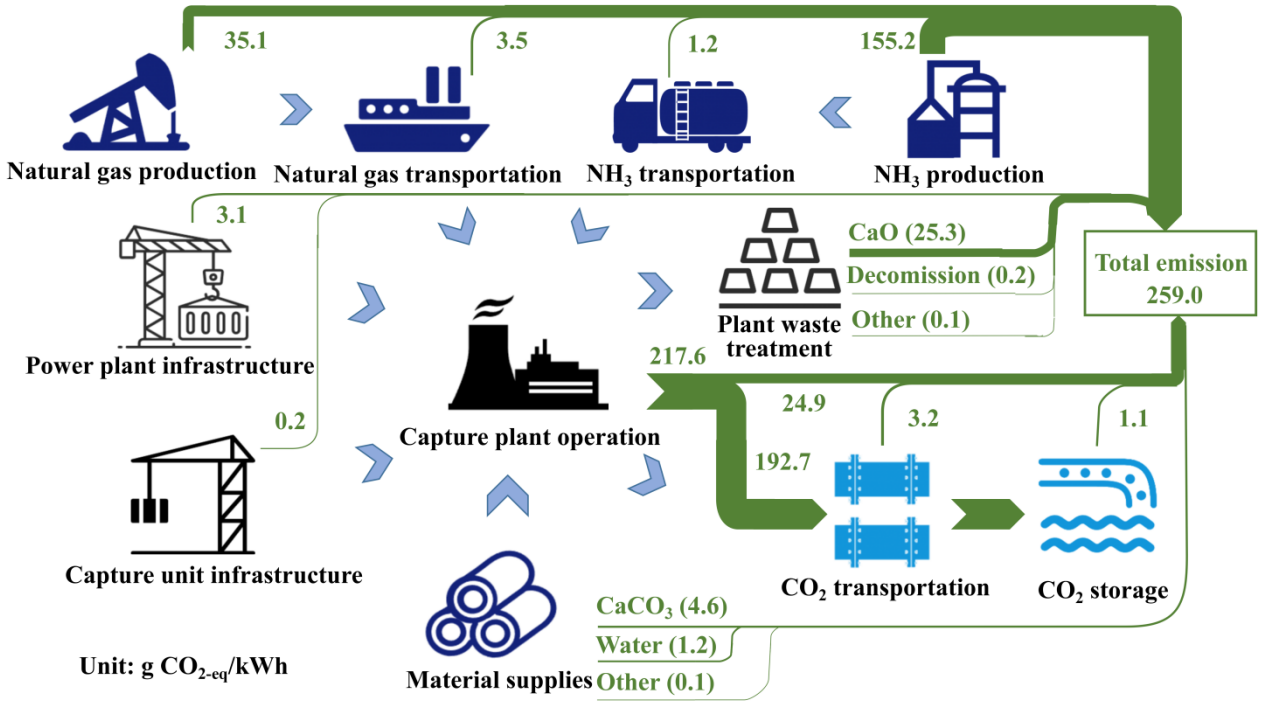

Fig.15 Carbon footprint of the CaL-NH_3-PV system

4.3 Life cycle cost assessment

The calculation assumption of direct and indirect costs of the plant configuration for life cycle cost is listed in Table S4 in the Supplementary Document, and the investment assumptions for

equipment based on the scaling factor method are provided in Table S5. And the calculated equipment costs for each CaL technology pathway can be found in Tables S10-S11. The main assumptions for economic calculations are listed in Table 6. The natural gas price used is the local rate, approximately 0.42 \$/Nm^3, and the CO_2 transportation cost and CO_2 storage cost are assumed to be 1.6 \$/t CO_2 and 5 \$/t CO_2, respectively.

Table 6 Main assumptions for the economic analysis

Items	Value	Ref.
NG price (\$/Nm^3)	0.42	[55]
X_{OM}	0.04	[56]
discount rate (%), *i*	12	[56]
Annual operation time, hours	4000	[55]
Equipment operation life (years), n	30	[56]
Green NH_3 price, (\$/t)	528	[57]
Ammonia cracking catalyst price, (\$/kg)	24.6	[58]
Catalyst lifetime (years)	5	[58]
$CaCO_3$ price, (\$/t)	22.4	[56]
CaO disposal cost, (\$/t)	11.2	[59]
CO_2 transportation cost, (\$/t CO_2)	1.6	[60]
CO_2 storage cost, (\$/t CO_2)	5	[61]

4.3.1 Economic results

Fig.16 shows the results of Levelized Cost of Electricity (*LCOE*). After integrating CaL technologies, the electricity generation cost increases by 50% to 60%. The *LCOE* values among the three systems are quite close, with the CaL-OXY system having the highest at 0.245 \$/kWh, followed closely by the CaL-NH_3 system at 0.239 \$/kWh, while the CaL-SOL system has the lowest cost at 0.236 \$/kWh.

The high cost of the CaL-OXY system is attributed to the notable decrease in efficiency compared to NGCC, leading to a higher operation costs and a substantial increase in *LCOE.* Conversely, the CaL-NH_3 system benefits from relatively lower efficiency penalties compared to the CaL-OXY system, resulting in a lower *LCOE*. It is worth noting that despite the higher energy penalties of the CaL-SOL

system, its economic performance shows a sightly advantage due to the free availability of solar resources. This offsets some of the efficiency drawbacks, making it a more cost-effective option in terms of long-term operational expenses.

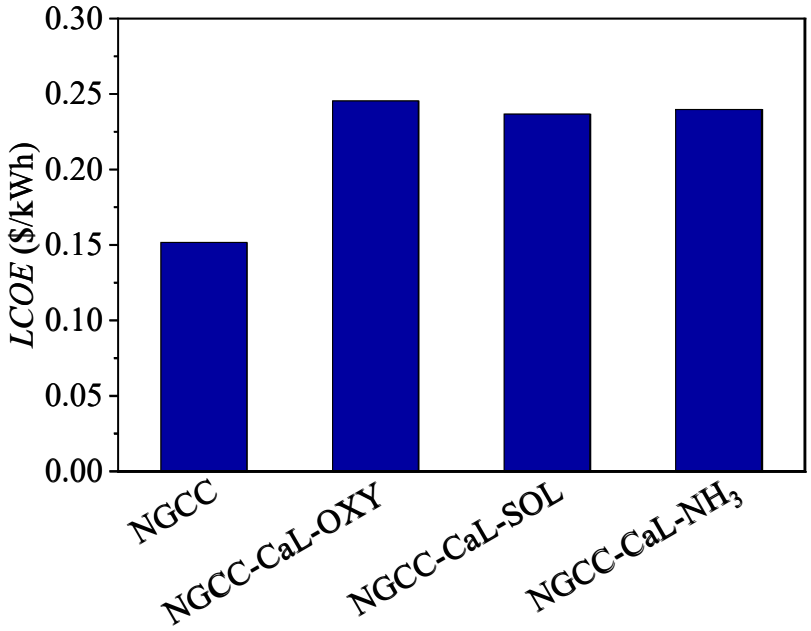

Fig.16 *LCOE* results for NGCC and NGCC capture plants with an annual operation time of 4000 hours

Fig.17 further compares the results of *COR* and *LCOR* for different technology pathways. COR is calculated based on the actual amount of CO_2 captured, while *LCOR* is based on the life cycle CO_2 avoided. The results indicate that, despite the highest *LCOE* of the CaL-OXY system, both COR and *LCOR* becomes lower, especially lower than that of the CaL-NH_3-PV system. This discrepancy primarily arises from differences in CO_2 capture and avoidance amounts. For the CaL-OXY system, the main CO_2 emissions come from the consumption of carbon-intensive fossil fuels, while the other two pathways incorporate renewable energy sources, reducing the carbon content input into the system. As a result, the *COR* and *LCOR* for systems utilizing renewable energy become higher for per unit of CO_2. It is also notable that *COR* and *LCOR* exhibit different relative trends across the technologies. For the CaL-OXY system, the CO_2 captured per unit of electricity is 0.46 t/MWh, which is higher than the life cycle CO_2 avoided per unit of electricity at 0.30 t/MWh. This is because the life cycle assessment includes emissions from the initial construction, production, and eventual decommissioning stages, resulting in higher *LCOR* compared to *COR*, at 308.4 \$/t CO_2 and 204.2 \$/t CO_2, respectively. In contrast, for the CaL-SOL and CaL-NH_3 systems, the CO_2 captured per unit of electricity is lower than the life cycle CO_2 avoided per unit of electricity. This is due to several factors:

the replacement of fossil fuels with solar energy and ammonia reduces the amounts of CO_2 captured, while the remaining energy is used to drive waste heat boilers for electricity generation, significantly increasing the electricity output. Consequently, the CO_2 capture per unit of electricity decreases substantially. Compared to the CaL-OXY system, the *COR* for the CaL-SOL and CaL-NH_3 systems increases by 32.4% and 124.1%, respectively, and the *LCOR* decreases by 19.7% and increases by 15.9%, respectively.

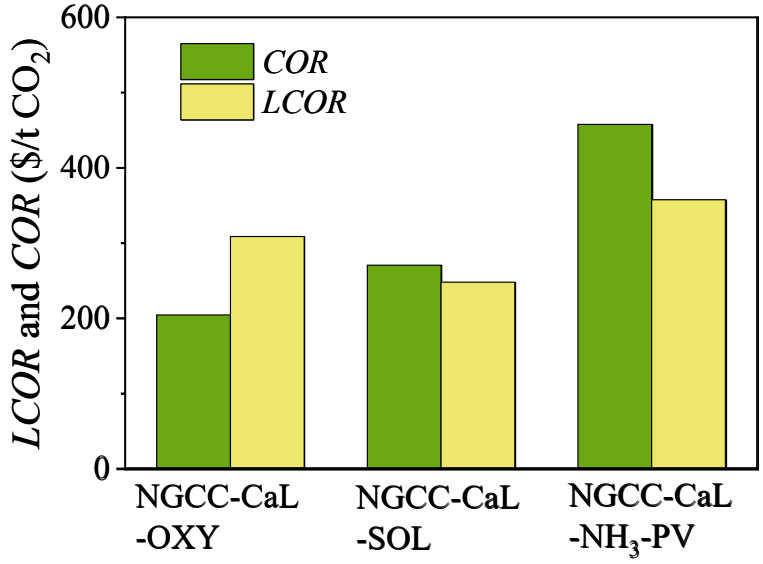

Fig.17 *LCOR* and *COR* results for NGCC capture plants with an annual operation time of 4000 hours

4.3.2 Sensitive analysis

Considering the significantly impact of fuel costs on life cycle economics, Fig.18 further examines how natural gas prices and green ammonia prices affect the *LCOR* for various technologies. The natural gas price is based on the Chinese market, where it fluctuates within the range of 2 to 4 CNY/Nm^3. This price is converted to USD based on the current exchange rate and then rounded. The results show differing effects of natural gas prices on the *LCOR* for each technology. For the CaL-OXY system, which relies mainly on natural gas, the LCOR increases as natural gas prices rise. When the price drops to 0.25 \$/Nm^3 , the *LCOR* is 284.8 \$/t CO_2. Conversely, for the CaL-SOL and CaL-NH_3 systems, *LCOR* increases as natural gas prices fall. This is because lower natural gas prices reduce the electricity generation costs of NGCC power plants, which in turn magnifies the influence of factors such as solar field investment and ammonia prices on the *LCOR*.

For the CaL-NH_3-PV system, considering that the current natural gas price is around 0.42 \$/Nm^3

in Chinese market, it is only competitive compared to the CaL-OXY system if the ammonia price drops below 450 $/t. Additionally, according to literature predictions, the green ammonia price is expected to decrease to 240 $/t by 2050 [62]. It can be observed that when the green ammonia price drops to 240 $/t, the CaL-$NH_3$ system demonstrates a clear economic advantage across the reasonable range of natural gas price fluctuations. If the natural gas price is 0.6 $/$Nm^3$, the *LCOR* for CaL-OXY, CaL-SOL, and CaL-NH_3-PV systems would be 334.5 $/t CO_2, 223.1 $/t CO_2, and 46.5 $/t CO_2, respectively. In this scenario, the CaL-NH_3-PV system shows a significant economic advantage, making it a more viable and cost-effective option in the long term for carbon capture and storage technologies.

Thus, from a life cycle economic perspective, the CaL-SOL system shows a competitive advantage at this stage, while the CaL-NH_3 system is expected to gain a significant advantage as ammonia prices decrease in the future, especially when natural gas prices are high.

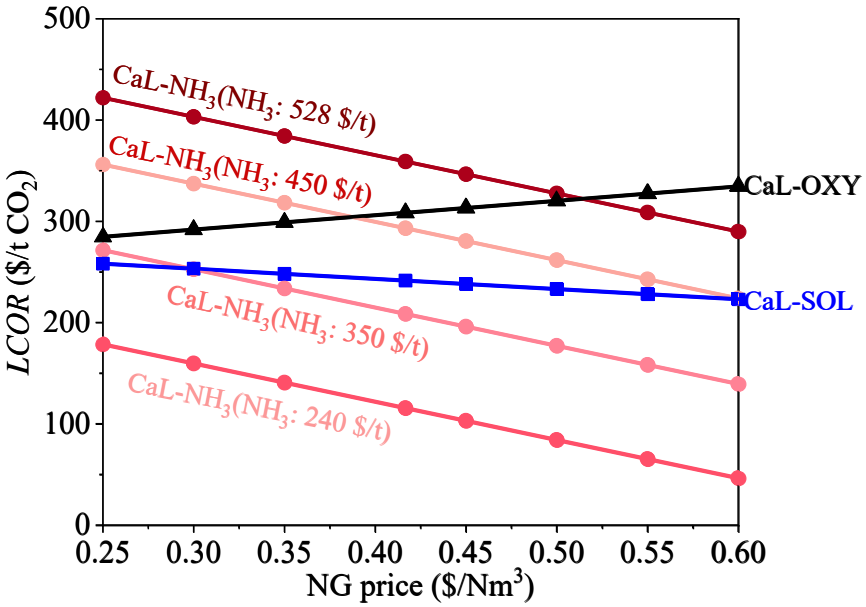

Fig.18 Sensitivity analysis of NG and green NH_3 prices on *LCOR* (NG price ranging from 0.25 $/t to 0.6 $/t, and green NH_3 price ranging from 240 $/t (predicted in 2050) to 240 $/t)

5. Conclusions

This paper proposes a novel NH_3-driven CaL process with thermochemical recuperation method, and compares its energy, life cycle environmental, and economic performances with oxy-fuel and solar-driven CaL systems for the carbon capture in existing NGCC plants. Some conclusions can be drawn as follows:

(1) The NH_3-driven CaL process demonstrates the highest energy efficiency, with an energy penalty of only 2.6 points, which is attributed to the superior integration between the calcium looping

process and chemical energy of heating fuel. Conversely, the solar-driven CaL method faces the highest energy penalty of 14 points due to the lower solar thermal conversion efficiency. And the use of renewable energy in the CaL unit enhances green power penetration, leading to a lower carbon emission intensity at 31.0 (solar) and 21.4 g CO_2-eq/kWh (NH_3).

(2) The NH_3-driven CaL method significantly impacts the environment more than oxy-fuel and solar-driven methods, with global warming potential values of 207.7 g CO_2-eq/kWh for the oxy-fuel CaL method, 170.7 for the solar-driven method, and 258.8 g CO_2-eq/kWh for the NH_3-driven method (PV based). When ammonia is sourced from wind power and biomass, the overall environmental performance improves compared to other sources. And the solar-driven CaL method has the least negative environmental impact.

(3) Economically, the solar-driven CaL system has the lowest *LCOE* and *LCOR* at 0.236 \$/kWh and 247.7 \$/t CO_2, respectively. With anticipated reductions in ammonia prices (in the future or using abandoned wind and solar power for production at present), the NH_3-driven CaL method could become more competitive, especially when natural gas prices rise. Specially, when the ammonia price drops to 240 \$/t, if the natural gas price is 0.6 \$/Nm^3, the *LCOR* for oxy-fuel CaL, solar-driven, and NH_3-driven methods would be 334.5 \$/t CO_2, 223.1 \$/t CO_2, and 46.5 \$/t CO_2, respectively.

Thus, from a life cycle environmental and economical perspective, the CaL-SOL system shows a competitive advantage at this stage, while the CaL-NH_3 system is expected to gain a significant advantage in economic as ammonia prices decrease in the future, especially when natural gas prices are high. At the same time, attention should be paid to the clean production process of ammonia to reduce its impact on the environment, such as the use of environmentally friendly materials, the improvement of energy efficiency in production processes and the use of clean energy.

CRediT authorship contribution statement

Yawen Zheng: Data curation, Formal analysis, Investigation, Writing - original draft, Funding acquisition. **Song He:** Conceptualization, Investigation, Methodology, Software, Writing - review & editing. **Jianhui Liu:** Funding acquisition, Writing - review & editing. **Junyao Wang:** Funding acquisition, Resources, Writing - review & editing. **Mingming Zhu:** Conceptualization, Writing - review & editing. **Guang Yang:** Writing - review & editing. **Wenxiang Wang:** Writing - review & editing.

Acknowledgements

This work was supported by China Postdoctoral Science Foundation (No. 2024M752134) and China Postdoctoral Science Foundation (No. 2024T170587), Shenzhen Science and Technology Program (KCXFZ20240903093459001) and Natural Science Foundation of Guangdong Province (No. 2024A1515012661).

Reference

[1] EIA, Electric Power Annual 2022, Washington 2023.

[2] IEA, World Energy Outlook 2021, 2021.

[3] A. Perejón, L.M.R. , Y.L. , P.L. , A.M. , J.M.V. , The Calcium-Looping technology for CO_2 capture: On the important roles of energy integration and sorbent behavior, Applied Energy, 162 (2016) 787-807.

[4] M. Heidari, M.T. , S.B.M. , C.P. , CO_2 capture activity of a novel CaO adsorbent stabilized with (ZrO_2+Al_2O_3+CeO_2)-based additive under mild and realistic calcium looping conditions, Journal of CO_2 Utilization, 53 (2021) 101747.

[5] E.D. Lena, M.S. , M.G. , R.S. , S.C. , S.C. , G.C. , M.C.R. , Techno-economic analysis of calcium looping processes for low CO_2 emission cement plants, International Journal of Greenhouse Gas Control 82 (2019) 244–260, 82 (2019) 244-260.

[6] Jian Chen, Lunbo Duan, Yuxin Ma, Yuxin Jiang, Anqi Huang, Hongyu Zhu, Hongyu Jiao, Mingdi Li, Yanbin Hu, Hui Zhou, Yongqing Xu, Felix Donat, Muhammad Awais Naeem, O. Krocher, Recent progress in calcium looping integrated with chemical looping combustion (CaL-CLC) using bifunctional CaO/CuO composites for CO_2 capture: A state-of-the-art review, Fuel, 334 (2023) 126630.

[7] J. Hilz, M.H. , M.H. , N.L. , J.S. , B.E. , Scale-up of the carbonate looping process to a 20 MWth pilot plant based on long-term pilot tests, International Journal of Greenhouse Gas Control, 88 (2019) 332–341.

[8] M. Haaf, J.P. , J.H. , A.U. , J.S. , B.E. , Combustion of solid recovered fuels within the calcium looping process – Experimental demonstration at 1 MWth scale, Experimental Thermal and Fluid Science, 113 (2020) 110023.

[9] M. Hornberger, J.M. , M.S. , G.S. , Experimental investigation of the calcination reactor in a tail-end calcium looping configuration for CO_2 capture from cement plants, Fuel, 284 (2021) 118927.

[10] B. Arias, Y.A.C. , A.M. , P.M. , I.F. , J.C.A. , Pilot Testing of Calcium Looping at TRL7 with CO_2 Capture

Efficiencies toward 99%, Energy & Fuels, 38 (2024) 14757−14764.

[11] R. Han, Y.W. , S.X. , C.P. , Y.H. , C.S. , Q.L. , Progress in reducing calcination reaction temperature of Calcium-Looping CO2 capture technology: A critical review, Chemical Engineering Journal, 450 (2022) 137952.

[12] M. Strojny, P. Gładysz, D.P. Hanak, W. Nowak, Comparative analysis of CO_2 capture technologies using amine absorption and calcium looping integrated with natural gas combined cycle power plant, Energy, 284 (2023) 128599.

[13] D. Berstad, R. Anantharaman, R. Blom, K. Jordal, B. Arstad, NGCC post-combustion CO_2 capture with Ca/carbonate looping: Efficiency dependency on sorbent properties, capture unit performance and process configuration, International Journal of Greenhouse Gas Control, 24 (2014) 43-53.

[14] D. Berstad, R. Anantharaman, K. Jordal, Post-combustion CO_2 capture from a natural gas combined cycle by CaO/CaCO3 looping, International Journal of Greenhouse Gas Control, 11 (2012) 25-33.

[15] Y. Hu, H. Ahn, Process integration of a Calcium-looping process with a natural gas combined cycle power plant for CO_2 capture and its improvement by exhaust gas recirculation, Applied Energy, 187 (2017) 480-488.

[16] H.D.P. Erans María, Mir Jordi, Anthony Edward J., Manovic Vasilije., Process modelling and techno-economic analysis of natural gas combined cycle integrated with calcium looping, Thermal Science, Volume 20 (2016) 59-67.

[17] C.-C. Cormos, Techno-economic assessment of calcium and magnesium-based sorbents for post-combustion CO_2 capture applied in fossil-fueled power plants, Fuel, 298 (2021) 120794.

[18] C. Fu, S. Roussanaly, K. Jordal, R. Anantharaman, Techno-Economic Analyses of the $CaO/CaCO_3$ Post-Combustion CO_2 Capture From NGCC Power Plants, 2 (2021).

[19] E. De Lena, B. Arias, M.C. Romano, J.C. Abanades, Integrated Calcium Looping System with Circulating Fluidized Bed Reactors for Low CO2 Emission Cement Plants, International Journal of Greenhouse Gas Control, 114 (2022) 103555.

[20] M. Greco-Coppi, P. Seufert, C. Hofmann, A. Rolfe, Y. Huang, S. Rezvani, J. Ströhle, B. Epple, Efficient CO_2 capture from lime plants: Techno-economic assessment of integrated concepts using indirectly heated carbonate looping technology, Carbon Capture Science & Technology, 11 (2024) 100187.

[21] R. Zhai, C. Li, J. Qi, Y. Yang, Thermodynamic analysis of CO_2 capture by calcium looping process driven by coal and concentrated solar power, Energy Conversion and Management, 117 (2016) 251-263.

[22] X. Zhang, Y. Liu, Performance assessment of CO_2 capture with calcination carbonation reaction process driven by coal and concentrated solar power, Applied Thermal Engineering, 70 (2014) 13-24.

[23] S. Khosravi, S. Hossainpour, H. Farajollahi, N. Abolzadeh, Integration of a coal fired power plant with calcium looping CO_2 capture and concentrated solar power generation: Energy, exergy and economic analysis, Energy, 240 (2022) 122466.

[24] D. Ferrario, S. Stendardo, V. Verda, A. Lanzini, Solar-driven calcium looping system for carbon capture in cement plants: Process modelling and energy analysis, Journal of Cleaner Production, 394 (2023) 136367.

[25] G. Moumin, M. Ryssel, L. Zhao, P. Markewitz, C. Sattler, M. Robinius, D. Stolten, CO_2 emission reduction in the cement industry by using a solar calciner, Renewable Energy, 145 (2020) 1578-1596.

[26] R. Zhai, C.L. , J.Q. , Y.Y. , Thermodynamic analysis of CO_2 capture by calcium looping process driven by coal and concentrated solar power, Energy Conversion and Management 117 (2016) 117 (2016) 251–263.

[27] S. Khosravi, S.H. , H.F. , N.A. , Integration of a coal fired power plant with calcium looping CO_2 capture and concentrated solar power generation: Energy, exergy and economic analysis, Energy, 240 (2022) 122466.

[28] D. Ferrario, S.S. , V.V. , A.L. , Solar-driven calcium looping system for carbon capture in cement plants: Process modelling and energy analysis, Journal of Cleaner Production, 394 (2023) 136367.

[29] C. Tregambi, F.M. , P.S. , R.S. , A model of integrated calcium looping for CO_2 capture and concentrated solar power, Solar Energy, 120 (2015) 208–220.

[30] C. Tregambi, P.B. , E.M. , F.P. , F.M. , R.S. , P.S. , Modelling of a concentrated solar power – photovoltaics hybrid plant for carbon dioxide capture and utilization via calcium looping and methanation, Energy Conversion and Management, 230 (2021) 113792.

[31] G. Colelli, R.C. , C.O. , A.C. , A.P.A. , V.V. , Life cycle and environmental assessment of calcium looping (CaL) in solar thermochemical energy storage, Energy Conversion and Management, 257 (2022) 115428.

[32] M. Strojny, P. Gładysz, D.P. Hanak, W. Nowak, Comparative analysis of CO_2 capture technologies using amine absorption and calcium looping integrated with natural gas combined cycle power plant Energy 284 (2023) 128599.

[33] D. Berstada, R. Anantharamana, R. Blomb, K. Jordal, B. Arstad, NGCC post-combustion CO_2 capture with Ca/carbonate looping: Efficiency dependency on sorbent properties, capture unit performance and process configuration, International Journal of Greenhouse Gas Control, 24 (2014) 43-53.

[34] S. He, Y. Zheng, X. Zeng, J. Wang, L. Gao, D. Yang, Proposal and thermodynamic investigation of pressurized calcium looping integrated with chemical looping combustion for tail-end CO_2 capture in a retrofitted natural gas combined cycle power plant, Separation and Purification Technology, 346 (2024) 127464.

[35] D. Lim, A. Kim, S. Cheon, M. Byun, H. Lim, Life cycle techno-economic and carbon footprint analysis of H_2

production via NH_3 decomposition: A Case study for the Republic of Korea, Energy Conversion and Management, 250 (2021) 114881.

[36] X. Zhang, P. Song, L. Jiang, Performance evaluation of an integrated redesigned coal fired power plant with CO_2 capture by calcium looping process, Applied Thermal Engineering, 170 (2020) 115027.

[37] W. Schakel, C.R. Hung, L.A. Tokheim, A.H. Stromman, E. Worrell, A. Ramírez, Impact of fuel selection on the environmental performance of post-combustion calcium looping applied to a cement plant, APPLIED ENERGY, 210 (2018) 75-87.

[38] S. Pascual, P. Lisbona, M. Bailera, L.M. Romeo, Design and operational performance maps of calcium looping thermochemical energy storage for concentrating solar power plants, Energy, 220 (2021) 119715.

[39] J. Dickmeis, A. Kather, The Coal-fired Oxyfuel-process with Additional Gas Treatment of the Ventgas for Increased Capture Rates, Energy Procedia, 63 (2014) 332-341.

[40] M. van der Spek, N.H. Eldrup, R. Skagestad, A. Ramirez, Techno-economic Performance of State-of-the-Art Oxyfuel Technology for Low-CO_2 Coal-fired Electricity Production, Energy Procedia, 114 (2017) 6432-6439.

[41] D. Pashchenko, R. Mustafin, I. Karpilov, Ammonia-fired chemically recuperated gas turbine: Thermodynamic analysis of cycle and recuperation system, Energy, 252 (2022) 124081.

[42] Z. Huang, B. Su, Y. Wang, S. Yuan, Y. Huang, L. Li, J. Cai, Z. Chen, A novel biogas-driven CCHP system based on chemical reinjection, Energy, 297 (2024) 131238.

[43] Y. Zheng, L. Gao, S. He, Analysis of the mechanism of energy consumption for CO_2 capture in a power system, Energy, 262 (2023).

[44] D. Jiang, S.L. , A.S.-A. , M.J. , Aspen plus-based techno-economic assessment of a solar-driven calcium looping CO_2 capture system integrated with CaO sorbent reactivation, Energy Conversion and Management: X, 23 (2024) 100673 (2024) 100673.

[45] C. Wang, S. He, L. Liu, X. Li, L. Gao, Tradeoff between the efficiency penalty and load depth in a coal-fired power plant with CO2 capture under partial load conditions, Energy Conversion and Management, 278 (2023) 116608.

[46] B. Ali, A.K. , Development of life cycle water footprints for gas-fired power generation technologies, Energy Conversion and Management 110 (2016) 110 (2016) 386–396.

[47] A. Ataei, I. , A, R. , Z., Life Cycle Assessment of Advanced Zero Emission Combined Cycle Power Plants, International Journal of Environmental Research, 6 (2012) 801-814.

[48] Y. Mozzhegorova, G.I. , V.K. , Life Cycle Assessment of a Gas Turbine Installation, Energies, 17 (2024) 345.

[49] V. Singh, I.D. , M.A.R. , Life cycle assessment of ammonia production methods, 2018.

[50] C. Wildbolz, Life Cycle Assessment of Selected Technologies for CO_2 Transport and Sequestration, Swiss Federal Institute of Technology Zurich, 2007.

[51] K. Damen, The Merits, Costs and Risks of Carbon Dioxide Capture and Storage, Utrecht University, 1977.

[52] P. Cui, D.Y. , Z.M. , Y.S. , X.L. , K.L. , Z.Z. , Z.L. , J.G. , Y.W. , S.Y. , Life cycle water footprint comparison of biomass-to-hydrogen and coal-to-hydrogen processes, Science of the Total Environment, 773 (2021) 145056.

[53] J. Lu, J.T. , R.S. , G.L. , P.R. , N.Z. , Spatiotemporal analysis of the future carbon footprint of solar electricity in the United States by a dynamic life cycle assessment, iScience, 26 (2023) 106188.

[54] Y. Zheng, S.H. , J.L. , X.Z. , B.X. , W.W. , G.Y. , Ammonia-enhanced calcium looping for carbon reduction in natural gas combined cycle plants, Applied Thermal Engineering 271 (2025) 271 (2025) 126245.

[55] Y. Zheng, J.W. , J.L. , S.H. , X.Z. , D.Y. , G.Y. , L.L. , Tracing the carbon capture energy distribution in a natural gas combined cycle power plant under variable operating conditions, Applied Thermal Engineering 246 (2024) 123000.

[56] S. He, L.G. , Y.Z. , J.W. , S.L. , Z.Y. , X.Z. , Carbonation heat recovery via dry reforming to improve the techno-economic performance of the Ca-Cu looping post-combustion CO_2 capture, Journal of CO_2 Utilization, 92 (2025) 103014.

[57] M. El-Shafie, S.K. , S.P.K. , S.N.P. , K.L. , Techno-economic study and process simulation for a small-scale hydrogen production plant based on ammonia decomposition, International Journal of Hydrogen Energy, 65 (2024) 126–141.

[58] C. Makhloufi, N.K. , Large-scale decomposition of green ammonia for pure hydrogen production, international journal of hydrogen energy 46 (2021) 34777-34787.

[59] C.-C. Cormos, Economic evaluations of coal-based combustion and gasification power plants with post-combustion CO_2 capture using calcium looping cycle, Energy, 78 (2014) 665-673.

[60] S.T. McCoy, The Economics of CO_2 Transport by Pipeline and Storage in Saline Aquifers and Oil Reservoirs, Carnegie Mellon University, USA, 2008.

[61] Y. Zheng, L.G. , S.L. , D.W. , A comprehensive evaluation model for full-chain CCUS performance based on the analytic hierarchy process method, Energy, 239 (2022) 122033.

[62] IEA, Ammonia Technology Roadmap, 2021.

https://dspace.org/

Life cycle analysis of ammonia-driven calcium looping processes for post-combustion CO2 capture in NGCC power plants

Zheng, Yawen; He, Song; Liu, Jianhui; Wang, Junyao; Zhu, Mingming ...

2025-08
Elsevier
https://doi.org/10.1016/j.jenvman.2025.126223
Zheng Y, He S, Liu J, et al., (2025) Life cycle analysis of ammonia-driven calcium looping processes for post-combustion CO2 capture in NGCC power plants. Journal of Environmental Management, Volume 390, August 2025, Article number 126223

Downloaded from a DSpace repository. https://dspace.org/